VISUAL ABSTRACT

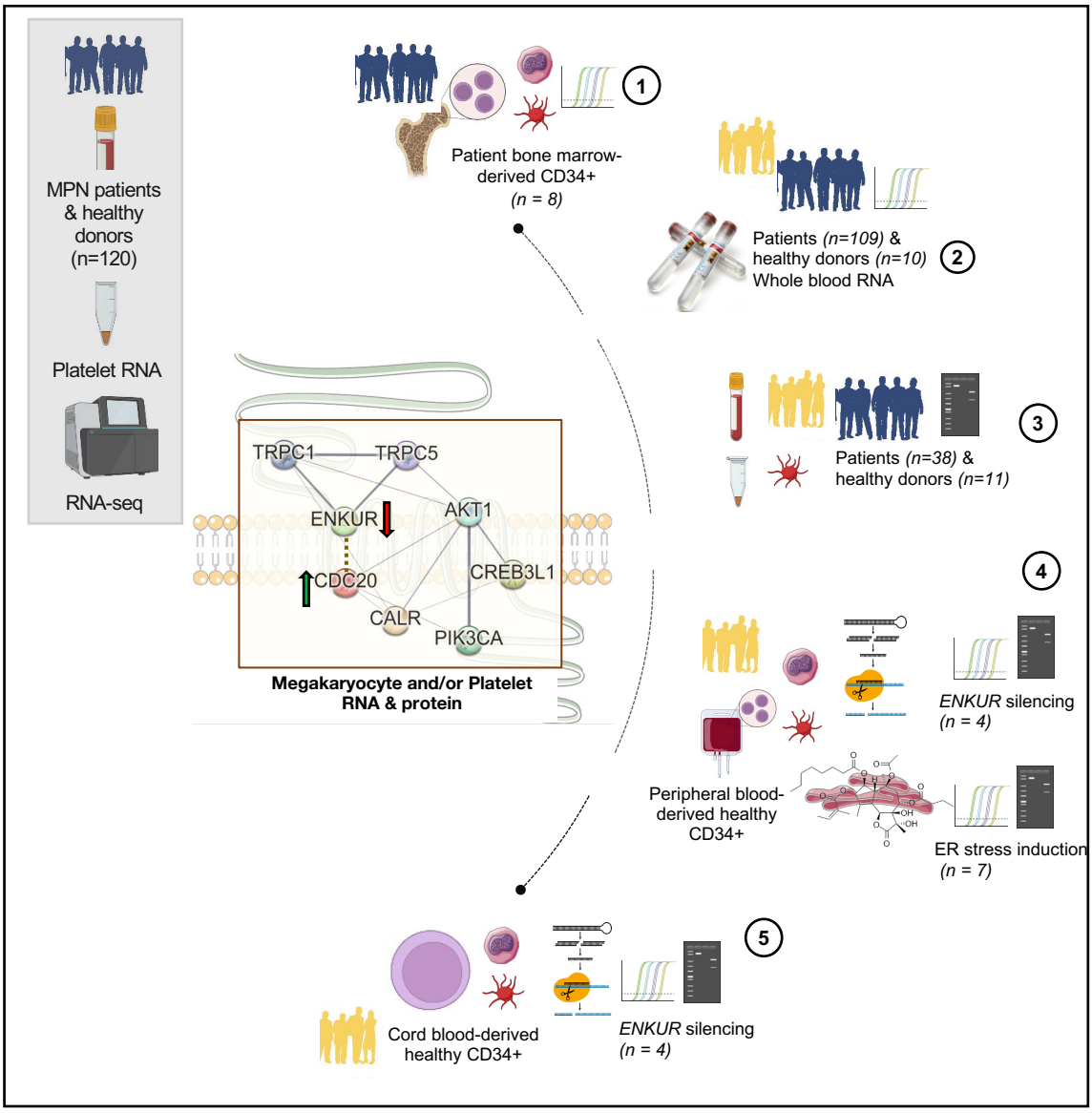

Enkurin: A novel marker for myeloproliferative neoplasms from platelet, megakaryocyte, and whole blood specimens.

Sumanth Mosale Seetharam[1#], Yi Liu[2#], Jason Wu[3], Lenn Fechter[4], Kanagavel Murugesan[1], Holden Maecker[4,5], Jason Gotlib[4,6#], James Zehnder[1,4,6#], Ramasamy Paulmurugan[2] and Anandi Krishnan[1,4*]

[1]Department of Pathology, Stanford University, Stanford, CA

[2]Department of Radiology, Stanford University, Stanford, CA

[3]High-Throughput Bioscience Center (HTBC), Stanford University School of Medicine, Stanford, CA

[4]Stanford Cancer Institute, Stanford University School of Medicine, Stanford, CA

[5]Department of Microbiology & Immunology, Stanford University School of Medicine, Stanford, CA

[6]Department of Medicine, Stanford University School of Medicine, Stanford, CA

[#]These authors contributed equally

[*]Correspondence: anandi.krishnan@stanford.edu

Key Points

1. Enkurin, a calcium adaptor protein, is identified as a novel marker of pathogenesis in MPNs.
2. MPN megakaryocyte and platelet expression of enkurin at RNA and protein levels is inversely associated with a cell differentiation cycle gene, CDC20.
3. Likely role for dysregulated calcium homeostasis, and ER and protein folding stress in MPN transformation.

Abstract

Impaired protein homeostasis, though well established in age-related disorders, has been linked in recent research with the pathogenesis of myeloproliferative neoplasms (MPNs). As yet, however, little is known about MPN-specific modulators of proteostasis, thus impeding our ability for increased mechanistic understanding and discovery of additional therapeutic targets. Loss of proteostasis, in itself, is traced to dysregulated mechanisms in protein folding and intracellular calcium signaling at the endoplasmic reticulum (ER). Here, using *ex vivo* and *in vitro* systems (including *CD34*$^{+}$ cultures from patient bone marrow, and healthy cord/peripheral blood specimens), we extend our prior data from MPN patient platelet RNA sequencing, and discover select proteostasis-associated markers at RNA and/or protein levels in each of platelets, parent megakaryocytes, and whole blood specimens. Importantly, we identify a novel role in MPNs for enkurin (*ENKUR*), a calcium mediator protein, implicated originally only in spermatogenesis. Our data reveal consistent *ENKUR* downregulation at both RNA and protein levels across MPN patient specimens and experimental models, with a concomitant upregulation of a cell cycle marker, *CDC20*. Silencing of *ENKUR* by shRNA in CD34^{+} derived megakaryocytes further confirm this association with *CDC20* at both RNA and protein levels; and indicate a likely role for the *PI3K/Akt* pathway. The inverse association of *ENKUR* and *CDC20* expression was further confirmed upon treatment with thapsigargin (an agent that causes protein misfolding in the ER by selective loss of calcium) in both megakaryocyte and platelet fractions at RNA and protein levels. Together, our work sheds light on enkurin as a novel marker of MPN pathogenesis beyond the genetic alterations; and indicates further mechanistic investigation into a role for dysregulated calcium homeostasis, and ER and protein folding stress in MPN transformation.

63 **Introduction**

64 Myeloproliferative neoplasms (MPNs) are a group of malignant disorders of the bone marrow where a
65 dysregulated balance between proliferation and differentiation gives rise to abnormal numbers of
66 blood cells in circulation. Classical MPNs[1,2] are defined by a combination of clinical, laboratory,
67 morphological and molecular genetic features, and constitute three phenotypic subtypes: essential
68 thrombocythemia (ET), polycythemia vera (PV), and myelofibrosis (MF, primary or secondary if
69 transformed from prior ET/PV). Somatic mutations in one of three driver genes (*JAK2, CALR, MPL*)
70 constitute their shared molecular genetic pathogenesis; causing constitutive JAK/STAT signaling in
71 hematopoietic stem cells (HSC)[3-7]. The mutated *CALR* also induces oncogenic effects by binding and
72 constitutively activating the thrombopoietin receptor and the downstream signaling cascade[7,8]
73 causing cellular transformation and abnormal megakaryopoiesis. To date, therapeutic strategies have
74 largely focused on *JAK2* inhibition (e.g. ruxolitinib[9]) and are effective in alleviating MPN symptoms,
75 but only partially, given their primary role in suppression of inflammation and reduction of
76 circulating pro-inflammatory cytokines[10,11]. Additional therapeutic strategies that target MPN
77 pathogenetic mechanisms[12-17] would be critical in resolving patient disease burden.

78

79 A recent study[18,19] assessing mechanisms of MPN pathogenesis identifies dysregulation of proteostasis
80 and protein quality control at the endoplasmic reticulum (ER) as crucial transformative events, and
81 therefore, a strong therapeutic target. However, this study was primarily in mice and remains to be
82 confirmed in independent additional MPN models and patient-derived specimens. Our recent
83 investigation, profiling the blood platelet transcriptome in all three subtypes of MPN patients[20]
84 identified high expression of genes and pathways associated with impaired proteostasis, ER stress and
85 unfolded protein response (UPR) well-recognized in other age-related disorders[21-25]. Here, we extend
86 our prior MPN patient platelet transcriptomic data with a focus on genes associated with proteostasis,
87 cell proliferation, ER stress or calcium signaling at high statistical significance (FDR <0.01), and
88 representing four types of trends in platelet RNA expression across MPN subtypes: progressively
89 downregulated, progressively upregulated, consistently upregulated, and uniquely upregulated in MF
90 alone. Genes selected include i) enkurin, *ENKUR*[26], a little-studied TRPC (transient receptor potential
91 cation channel[27,28]) adaptor protein with known function primarily in the context of sperm motility
92 alone[26,29], ii) *CALR, a* well-known ER chaperone and calcium binding protein[30-34], also relevant in the

93 context of megakaryocyte to platelet differentiation[35-38], iii) cyclic AMP-responsive element-binding
94 protein *CREB3L1,* an ER-Golgi stress transducer and transcription protein involved in the UPR
95 response[39-42] and lastly iv) *CDC20,* involved in cell division and proliferation[43-45], and known to be
96 upregulated in other cancers[45]. Using MPN patient bone marrow- and healthy cord- and peripheral
97 blood-derived CD34+ cells differentiated into megakaryocyte and platelet cultures *ex vivo*, we
98 consistently identify *ENKUR* as a novel peripheral and marrow biomarker in MPNs at both RNA and
99 protein levels. Our data also demonstrate a negative correlation of *ENKUR* with *CDC20* expression in
100 the megakaryocyte/platelet cultures, and in independent banked MPN whole blood RNA specimens.
101 Beyond the utility of enkurin as a potential marker of MPN chronic vs advanced subtypes, more
102 research is warranted to elucidate the mechanisms of its downregulation in MPNs, and how that may
103 target cell proliferation pathways.
104

105 **Methods**

106 Please see **Table 1** for a tabulated overview of all RNA and protein measurements in this study.

107 **Ethics Statement**

108 All MPN patient and healthy donor samples were obtained under written informed patient consent
109 and were fully anonymized. Study approval was provided by the Stanford University Institutional
110 Review Board. All relevant ethical regulations were followed.
111

112 **Materials**

113 We collected MPN patient bone marrow specimens from the Stanford Cancer Center, and whole
114 blood from healthy donors at the Stanford Blood Center. Cell culture supplies including plates, fetal
115 bovine serum, penicillin, streptomycin, phosphate-buffered saline (PBS), and culture medium were
116 procured from GIBCO BRL (Frederick, MD). Antibodies for CALR, CDC20, p-PI3K, p-Akt, b-Actin
117 and anti-rabbit goat IgG were procured from Cell Signaling Technologies (Danvers, MA), for enkurin
118 from Sigma Aldrich (St. Louis, MO) and CREB3L1 from Thermo Scientific (Rockford, IL). Antibodies
119 for Alexa647-tagged CD41, PE-CD42b, PE-CD61, and PE-CD45 were from BioLegend (San Diego,
120 CA). shRNA for ENKUR silencing were synthesized from Protein and Nucleic acid facility at
121 Stanford University (Stanford, CA). The human HEK 293 FT cells and THP1 human macrophage cells
122 were purchased from the American Type Culture Collection (ATCC, Manassas, VA) and cultured

123 following supplier instructions. The CD34, CD45 microbeads, LS and MS columns and magnetic
124 separators were purchased from Miltenyi Biotech (Cambridge, MA). Cytokines IL6, thrombopoietin
125 TPO, and Flt3 ligand were from PeproTech Inc. (Cranbury, NJ); SCF and SFEM II media was from
126 Stem Cell Technologies (Kent, WA). Lenti-X™ GoStix™ Plus was purchased from TaKaRa Bio Inc.
127 (San Jose, CA).
128

129 **Peripheral blood platelet isolation**

130 Peripheral blood was collected in acid citrate-dextrose (ACD, 3.2%) sterile yellow-top tubes (Becton,
131 Dickinson and Co.) and was processed within 4 h of collection for all samples. Platelets were isolated
132 by established[46-49] purification protocols. Briefly, the ACD-tube whole blood was first centrifuged at
133 200xg for 20min at room temperature (RT). The platelet-rich plasma (PRP) was removed and
134 Prostaglandin E1 was added to the PRP to prevent exogenous platelet activation. The PRP was then
135 centrifuged at 1000xg for 20min at RT. The platelet pellet was re-suspended in warmed (37 deg C)
136 PIPES saline glucose (PSG). Leukocytes were depleted using $CD45^+$ magnetic beads (Miltenyi Biotec).
137 Isolated platelets were further resuspended in Trizol or LDS buffer for RNA (PCR) and protein
138 (Western Blot) analyses.
139

140 **RNA extraction and quantification from whole blood (PAXgene tubes)**

141 Whole blood from MPN patients and healthy donors was collected into PAXgene tubes (BD
142 Biosciences) containing RBC lysis buffer . RNA was isolated using PAXgene Blood RNA kit following
143 manufacturer instructions (762164, PreAnalytix, Switzerland).
144

145 **$CD34^+$ cell isolation from MPN bone marrow and healthy peripheral and cord blood cultures**

146 $CD34^+$ cells were isolated[50,51] using microbeads positive selection (Miltenyi Biotec) from source
147 specimens of peripheral blood or cord blood of healthy donors or bone marrow of MPN patients
148 (collected as part of their clinical care with research consent). Briefly, the RBCs were lysed using
149 RBC lysis buffer and the cells pelleted. Cells were suspended in MACS running buffer and incubated
150 with the $CD34^+$ microbeads for 1 hour on ice and then passed through MACS LS columns pre-
151 equilibrated with MACS running buffer. $CD34^+$ cells thus collected were washed using MACS
152 running buffer and resuspended in the SFEM II media (4-5x10^5 cells/mL) containing TPO (20ng/ml),

153 SCF (25ng/ml) and Gentamicin (1:1000) and plated/transferred to 12 well plates at 37 °C in 5% CO_2.
154 On day 3, cells were resuspended in fresh media (SFEM II) containing TPO (20ng/ml), SCF (25ng/ml)
155 and Gentamicin (1:1000), and on day 6, 9, and 12, in TPO (40ng/ml) and Gentamicin (1:1000). The
156 cells were harvested on day 15. Cells were collected and centrifuged at 300xg for 10 min to pellet the
157 larger megakaryocyte fraction and at 3000xg for 30 min for the smaller platelet fraction. With both
158 peripheral- and cord-blood-derived $CD34^+$ cells, the isolated cells were expanded using hematopoietic
159 stem cell expansion media (Cell Genix) containing 100ng/ml of IL6, Flt3 ligand, SCF, and TPO for 5
160 days before starting the culture. The formation of MK cells and platelets were confirmed by surface
161 marker analysis with CD41, CD42b and CD61.
162

163 **Cell surface marker analysis using flow cytometry**

164 Following isolation of the megakaryocyte and platelet fractions from the 14-day (+TPO) $CD34^+$
165 culture, cells were collected and washed with PBS. For the CD41, CD42b and CD61 stains, cells were
166 resuspended in MACS running buffer and stained with Alexa 647 anti-human CD41, PE anti-human
167 CD42b, and PE anti-human CD61, and incubated at RT protected from light for 45 min. Cells were
168 washed with PBS and resuspended at a final concentration of 2×10^7 cells/ml in PBS, prior to running
169 the sample on the flow cytometer. All experiments were performed using GUAVA Flow Cytometer
170 and all flow cytometry analysis was performed in the FlowJo Software. Data from flow cytometry
171 experiments was acquired by gating for events that were in focus.
172

173 **Total RNA isolation and PCR with $CD34^+$ derived megakaryocyte and platelet fractions**

174 Total RNA was isolated from the megakaryocyte (MK) and platelet fractions using a mirVana RNA
175 extraction kit (Life Technologies, Grand Island, NY) in accordance with the manufacturer's
176 instructions. Briefly, MKs/platelets were homogenized into 300µl lysis buffer, then incubated with
177 30µl homogenate additive for 10 min. RNA was extracted with acid-phenol and column purified,
178 then washed three times with washing buffer, and eluted in 40µl of sterile elution buffer. The total
179 RNA was quantified first using a Nanodrop spectrophotometer, then 100ng of total RNAs were
180 reverse-transcribed using a Reverse-Transcription Kit (Life Technologies) and RT primers to
181 synthesize cDNA. Then, qRT-PCR was performed using the TaqMan-PCR primers and probe mix
182 combined with the cDNA derivates. qRT-PCR was performed through 2 min incubation at 50 °C,

183 then followed by DNA polymerase activation at 95 °C for 10 min; plus 60-cycles at 95 °C for 15 s, and
184 60 °C for 60 s in the BioRad CFX96 thermocycler system (BioRad). The qRT-PCR reaction procedure
185 was executed in a 20µl final reaction volume. The expression of target genes was analyzed by the
186 2–ΔΔCt method.
187
188 **Thapsigargin-induced ER stress**
189 Isolated human $CD34^+$ cells from the peripheral blood of healthy volunteers were cultured for 15
190 days with the supplementation of both SCF and TPO for the first 6 days and then with TPO alone till
191 day 15. Fresh media containing either SCF and/ or TPO was added every 3 days. To induce ER stress
192 in these cells, known ER stressor drug Thapsigargin (125nM, as optimum dosage identified via
193 preliminary experiments) was added to the culture on day 7. The culture was maintained till day 15
194 with media change every 3 days. The cells were harvested and analyzed for gene expression and
195 immunoblotting for the target proteins.
196
197 **Western Blotting for protein expression in megakaryocytes and platelets**
198 Isolated MKs were aliquoted for flow cytometry, RNA expression and western blotting. For western
199 blotting, an aliquot of the MK cells was pelleted and lysed using cell lysis buffer containing protease
200 inhibitor cocktail, EDTA. The samples were then resolved on a reducing SDS-PAGE (10%
201 acrylamide). Blots were stained using appropriate primary (anti-human rabbit antibody; 1:1000 v/v)
202 and secondary antibodies (anti-rabbit IgG HRP conjugate; 1:2000 v/v).
203 Protein expression was determined based on the detection of a band. The intensity of the protein
204 bands observed was semi-quantified using IVIS or ImageJ software with normalization of each
205 protein against beta-actin. Blots were visualized using ECL reagent by Amersham Imager 680 or by
206 IVIS imaging systems.
207
208 **ENKUR gene silencing**
209 **a. Construction of the vector**
210 PLKO1 vector was used to construct the ENKUR-silenced cell lines in HEK293T cells (known for
211 their ease of transfection and fast growth rate). The PLKO1 vector was cut using EcoR1 and Age1 to
212 ligate the shRNA using T4 ligase.

213 The shRNA sequences used were:

214 shRNA1: PCCGGTCCGGCCAACCTCGATACTCTTATTTCTCGAGAAATAAGAGTATCG

215 AGGTTGGTTTTTTTTGG

216 shRNA 2:

217 PCCGGTCCGGCATGGGAGTGGCTAAAAAGCCCTCGAGGGCTTTTTAGCC

218 ACTCCCATGTTTTTTTTGG

219 Scrambled: PCCGGTCCGGGTGCGTTGCTAGTACCAACTCTCGAGAGTTGGTACTA

220 GCAACGCACTTTTTTTTGG

221

222 **b. Validation of the construct**

223 The silencing effect of the shRNA construct was assessed using HEK293 FT cells by transfection of
224 the shRNA containing plasmids (pLKO1-shRNA) using lipofectamine method. Briefly, 100K HEK293
225 FT cells were seeded in a 12-well plate 24h prior to the transfection. Transfection was performed by
226 adding a master mix containing lipofectamine and the shRNA in reduced serum media for 4 hours,
227 before adding the complete media. The cells were harvested 48h after transfection and the silencing
228 effect assessed by western immunoblotting against enkurin.

229

230 **Cell culture for ENKUR silencing**

231 HEK293 FT cells were cultured in Dulbecco's Modified Eagle's Medium/high glucose with 10% FBS,
232 0.1% streptomycin, and 100 U mL^{-1} penicillin at 37 °C, 5% CO_2, and 95% air environment, while
233 THP-1 cells were cultured in RPMI media containing 10% FBS, 0.1% streptomycin, and 100 U mL–1
234 penicillin at 37 °C, 5% CO_2, and 95% air environment. The cells were tested for any mycoplasma
235 contamination using a MycoAlert kit (Lonza, Allendale, NJ), and were maintained at optimum
236 cultural conditions.

237

238 **Production of lentiviral particles**

239 After the confirmation of the silencing effect of the shRNA construct, they were packaged along with
240 the viral plasmids to produce the lentivirus. Briefly, the lentiviral vectors were transfected to HEK293
241 FT cells using calcium phosphate method. The cells were supplemented with chloroquine and
242 HEPES. After 48h of incubation, the media was carefully aspirated, and the viral particles were

243 concentrated by ultracentrifugation. The IFU value was determined by Lenti-X GoStix following
244 manufacturer instructions (Cat#631280).
245
246 **Validation of the lentivirus silencing in HEK cells**
247 As above, 100K HEK293 FT cells were plated in a 12-well plate 24h prior to lentiviral infection
248 (transduction). The media was aspirated and lentivirus master mix containing polybrene in reduced
249 serum media was added to the cells. After 4h of incubation, the cells were supplemented with
250 complete media and was incubated for 48h before harvesting. The cells were lysed and
251 immunoblotted against enkurin to assess the gene silencing effect.
252
253 **ENKUR gene silencing in $CD34^+$ derived megakaryocytes**
254 The shRNA expressing lentiviral particles were infected into the $CD34^+$ cells in culture on day 9 (MKs
255 derived from $CD34^+$ cells) at a ratio of 1:20 (cell: viral particle). The culture was maintained for
256 another 6 days with supplementation of TPO every 3 days. Cells were harvested on day 15; and
257 centrifuged at two speeds; low (300xg) and high (3000xg) to separate the MK and platelet fractions
258 respectively. Each fraction was divided into 3 aliquots for assessing each of cell surface markers (50 –
259 100K cells), RNA (~50K cells) and protein (100 – 200K cells) expression.
260
261 **Statistical Analyses**
262 Continuous variables from all experiments were assessed for normality. Data that were normally
263 distributed were expressed as a mean plus or minus the standard error of the mean. For analyses
264 involving two groups, a parametric two-tailed student t-test was used. When three or more groups
265 were analyzed, an ANOVA with a Tukey's post-hoc test was performed. When data were not
266 normally distributed a Mann-Whitney was used when two groups were analyzed while a Kruskal-
267 Wallis with a Dunn's multiple comparison post-hoc test was used for analyses of three or more
268 groups. When appropriate a two-way ANOVA with post-hoc test was used as described. Summary
269 statistics were used to describe the study cohort and clinical variables were expressed as the mean ±
270 error of the mean or as a number and percentage (%). Statistical analyses were performed by using
271 GraphPad Prism (version 9, San Diego, CA), and a p-value < 0.05 was considered statistically
272 significant.

273 **Results**

274 **Validation of RNA and protein expression of 4 MPN candidate markers**

275 Four candidate markers from our prior platelet RNA-seq analyses[20] were identified based on specific
276 trends in progressive expression across the 3 MPN subtypes vis-à-vis healthy donors (FDR<0.01,
277 n=120) independent of patient driver mutational status. *ENKUR and CALR*, in particular, were
278 identified based on opposing trends in progressive expression (**Figure 1A and Figure S1A**), *CDC20* on
279 its specific high expression in MF patients alone in contrast with healthy donors and ET or PV
280 patients (**Figure 1A,** top right), and *CREB3L1* based on its substantially increased (> 50-fold)
281 expression in all MPNs vs healthy (**Figure S1A,** top right). Given that the platelet RNA profile is a
282 composite of influences from the peripheral circulation as well as of the genetic (and MPN
283 mutational) profile of megakaryocytes in the bone marrow, we hypothesized *a priori* that our MPN
284 candidate markers are likely to be variably validated in one versus the other.

285

286 First, in whole blood RNA of MPN patients versus healthy donors, expression of *ENKUR* and *CDC20*
287 was confirmed by qPCR (**Figure 1B**, n=109, $p < 0.005$) as nearly 6-fold downregulated and 3-fold
288 upregulated respectively in the advanced MPN subtype, MF. Expression of *CREB3L1* was also
289 confirmed as over 15-fold upregulated across ET, PV, and MF (**Figure S1B,** right panel), whereas
290 expression of *CALR* (**Figure S1B,** left panel) was variable and not uniformly consistent with the
291 platelet transcriptome (likely owing to lower resolution for detection of transcripts in whole blood).
292 Next, in assessing platelet protein levels, trends in expression of ENKUR was significantly different in
293 PV and MF versus healthy donors, and CDC20 in ET and MF (**Figure 1C**), whereas CALR and
294 CREB3L1 were not significantly different between patient and healthy donor specimens (**Figure S1C**).

295

296 **Megakaryocyte and platelet fractions from CD34$^+$ cultures of MPN patient bone marrow**

297 To further delineate RNA expression of the candidate markers as specific to platelets in circulation
298 alone or also in marrow-derived megakaryocytes, we established an *ex vivo* culture of CD34$^+$ stem
299 cells from MPN patient bone marrow (n=8, 4 MF) and generated megakaryocyte and platelet
300 fractions (**Figure 2A-B**, and Methods and **Figure S2A-B** for flow cytometric and histological
301 confirmation of cultured megakaryocyte and platelet fractions). Given the variable differentiation
302 states of the nascent platelet fraction and its lower cell quantity than the megakaryocytic fraction, we

303 focused entirely on the megakaryocytes harvested. Downregulation of *ENKUR* was recapitulated in
304 these patient-derived megakaryocytic RNA (mean approx. 2-fold reduction in MF alone and 5-fold all
305 MPN) with associated upregulation of *CDC20,* CREB3L1 (mean of approx. 1-fold) and *CALR* (~4-
306 fold) in all MPN (n=8, **Figure 2C**).
307
308 ***ENKUR* gene silencing**
309 To better evaluate the negative correlation between *ENKUR* and *CDC20/CALR* expression, we
310 sought lentiviral knockdown in primary $CD34^+$ cells (derived from healthy peripheral blood and cord
311 blood specimens) using two distinct *ENKUR* shRNA constructs. **Figure 3A-B** describes our
312 experimental framework. The shRNAs were first expressed in pLKO.1 plasmid that was amplified and
313 isolated from *E.coli*, and the lentiviral plasmids were then transfected into HEK293 FT cells to
314 generate the lentivirus. *ENKUR* shRNA silencing and downregulation of enkurin protein was
315 confirmed at a concentration of 1:20 HEK cell:viral particle. Primary $CD34^+$ cells from healthy
316 peripheral (n=4) and cord blood (n=4) specimens were cultured at four conditions: i) control with no
317 ENKUR silencing, ii) *and* iii) lentiviral knockdown with the two shRNA constructs, and finally iv)
318 scramble control shRNA. Where relevant, shRNA infection was introduced at day 7 of culture and
319 continued for another 7 days (totaling a 15-day culture, **Figure 3B**). Megakaryocyte and platelet
320 fractions thus derived were confirmed by flow cytometric analysis (**Figure 4A**). Downregulated RNA
321 expression of *ENKUR* was significantly associated with concomitant high expression of *CDC20* in
322 both of the megakaryocyte and platelet fractions (**Figure 4B**). Cell quantity in the platelet fraction
323 was just sufficient for RNA qPCR measurements alone, and therefore, protein levels could be assessed
324 only in the megakaryocytes. Inverse correlation between ENKUR and CDC20 was validated even in
325 megakaryocytic protein expression (**Figure 4C).** However, *ENKUR* silencing alone (without the
326 associated patient factors in our *in vitro* experiments, e.g. mutational status) was insufficient to
327 generate a statistically significant differential in *CALR or CREB3L1* expression at both RNA and
328 protein levels (**Figure S3A-B**).
329
330 One classical downstream pathway linked previously to ER stress response[18,19] in MPNs[52] and other
331 cancers[53-55] is the PI3K/Akt signaling cascade. Here with shENKUR, we briefly evaluated possible

332 association with the PI3K/Akt pathway and found that silencing of enkurin correlated with increased
333 expression of phosphorylated PI3K in megakaryocytes (**Figure 4C**).
334
335 **Effect of ER stress on CD34$^+$-derived megakaryocytes**
336 Considering that the differential and inversely correlated expression of *ENKUR* and *CDC20* extends
337 to the CD34$^+$ cell-derived megakaryocytes, and our hypothesis on the role of ER stress in this
338 response, we assessed RNA and protein levels of these markers following treatment of the cells with
339 the sarco/endoplasmic reticulum Ca^{2+}-ATPase inhibitor, thapsigargin (125nM). CD34$^+$ cells from
340 peripheral blood of healthy donors were differentiated into megakaryocyte and platelet fractions,
341 with thapsigargin introduced at day 7 of a 15-day culture (see Methods and **Figure 5A**; limited cell
342 quantity of the platelet fraction enabled protein analyses in the megakaryocytic fraction alone).
343 Thapsigargin evoked a similar expression profile in megakaryocytes **(Figure 5B-C)** as that of MPN
344 patient bone marrow-derived CD34$^+$ cells with downregulated *ENKUR* and upregulated *CDC20*
345 expression at both RNA and protein levels.
346
347 **Discussion**
348 Here, we present the first report, to our knowledge, of enkurin (*ENKUR*) as a potential new
349 peripheral biomarker and therapeutic strategy in myeloproliferative neoplasms. Our prior study[20]
350 profiling the platelet transcriptome in patients with chronic MPNs (n=120) identified progressive
351 association in expression of several proteostasis-associated genes with advancing disease subtype. Our
352 findings were consistent with other studies demonstrating dysregulated proteostasis as a primary
353 effector of myeloid transformation[18,56,19,57]. The MPN platelet RNA-seq data also confirmed the limited
354 impact[58] of treatment by JAK2-inhibitor ruxolitinib (RUX) relative to the substantial disease burden
355 in myelofibrosis; and urged the need for development of novel candidate drugs to be used alone or in
356 combination with RUX for the treatment of MPNs.
357
358 Four candidate markers from the prior study (*ENKUR, CDC20, CALR, and CREB3L1*) were evaluated
359 in this work based not only on their significant association with pathways related to proteostasis, cell
360 proliferation, ER stress or calcium signaling, but also progressive increase or decrease in differential
361 expression across the MPN chronic vs advanced subtypes (ET/PV to MF versus healthy donors)

362 regardless of patient *JAK2/CALR* mutational status. Using CD34$^+$ cells isolated from MPN patient
363 bone marrow as well as healthy donor peripheral and cord blood, we generated *ex vivo*
364 megakaryocyte and platelet fractions and discovered at both RNA and protein levels, an inverse
365 correlation between *ENKUR*, a calmodulin and TRPC channel modulator[26,29] (not previously
366 associated with MPNs) and *CDC20* (also termed Fizzy[44]), a cell cycle gene and an anaphase promoting
367 complex activator (with known associations with malignancies broadly[43,59] and select studies in
368 MPNs[60]). Lentiviral-mediated silencing of *ENKUR* was utilized to further confirm the negative
369 association between *ENKUR* and *CDC20;* and indicating a potential interaction via the PI3K-Akt
370 pathway **(Figure 6)**. Our data on the inverse association between enkurin, a membrane calcium influx
371 adaptor protein, and *CDC20*, a crucial cell cycle and proliferation regulator point to a role for
372 dysregulated calcium signaling in MPNs; and the possibility for the ratio of expression between the
373 two to be developed as a potential biomarker of MPN disease.
374
375 Next, in evaluating calreticulin (*CALR*), a well-established driver mutation in MPNs[31,61], as well as
376 *CREB3L1*, an ER/UPR stress response transcription factor, high expression noted previously across
377 MPN patient platelet RNA-seq[20] was confirmed in patient-derived specimens (platelet, whole-blood,
378 and bone-marrow-CD34$^+$-cultured megakaryocytes) but only at the RNA (and not protein) levels.
379 Future investigations applying genome editing in MPN models will be needed to ascertain
380 overlapping mechanisms of somatic alterations in *CALR* and its effect on function in altered calcium
381 signaling and dysregulated ER protein folding[62,63] in MPNs.
382
383 Taken together, we offer two inversely associated MPN markers, *ENKUR* and *CDC20*, whose whole
384 blood, platelet and megakaryocyte RNA and protein expression reflect MPN pathobiology
385 irrespective of patient driver mutational status. These candidate markers also seek to expand our
386 understanding of MPN pathology beyond the classical inflammatory signatures[64-67].
387
388 **Limitations of the study**
389 There are several limitations to our study. First, higher statistical power and longitudinal prospective
390 data will be necessary to further confirm *ENKUR/CDC20* as markers for MPN disease progression.
391 Second, future investigations evaluating these signatures in patient-derived CD34$^+$ cells may identify

additional functional aspects of bone marrow and MPN pathology. Third, we recognize that our data are not assessing mechanistic signaling of how loss of *ENKUR* expression or impaired calcium signaling contributes to myeloproliferation; and will need to be specifically interrogated in MPN murine and other models. Follow-on studies evaluating a potential role of the *PI3K/Akt* pathway, in particular the effect of pharmaceutical inhibitors already in use in MF will add significant value to the current study. Studies evaluating platelet function under impaired enkurin expression and calcium modulation are promising immediate future directions. And above all, it will be important to assess how enkurin downregulation might be more broadly relevant to other hematological cancers, such as myelodysplastic syndromes and acute myeloid leukemia, or potentially unique to MPNs alone.

Acknowledgements

This work was funded by the MPN Research Foundation and the US National Institutes of Health grants 1K08HG010061-01A1 and 3UL1TR001085-04S1 (research re-entry award) to A.K. Other support included 1S10OD018220 and 1S10OD021763 shared instrumentation grants to the Stanford Functional Genomics Facility and the Stanford Research Computing Center, and the Charles and Ann Johnson Foundation to J.G. All authors thank the patients at the Stanford Cancer Center and the healthy donors at the Stanford Blood Center for their generous participation in this research, and the Canary Center at Stanford for Cancer Early Detection for access to flow cytometry and microscopy. Authors also thank Dr. Diwash Jangam for his assistance with the initial Paxgene PCR setup.

Author Contributions AK conceived of the study and the team, secured funding, and wrote the manuscript. LF and JG provided samples and clinical annotation and reviewed the clinical data. AK and RP coordinated and oversaw sample acquisition and processing. SS, YL, JW, and KM performed the experiments and interpreted the analyses with AK, RP, HM, JG, and JZ. All authors critically reviewed and edited the manuscript. [#]SS and YL contributed equally. [#]JG and JZ also contributed equally. All authors approved the final manuscript.

Conflict of Interest Disclosures: Authors declare no conflict of interest.

Bibliography

1. Tremblay, D., Yacoub, A., and Hoffman, R. Overview of Myeloproliferative Neoplasms: History, Pathogenesis, Diagnostic Criteria, and Complications. Hematol Oncol Clin North Am. 2021;35(2):159-176. Epub 2021/03/02. PubMed PMID: 33641861; PMCID: PMC8669599.
2. Arber, D.A., Orazi, A., Hasserjian, R., Thiele, J., Borowitz, M.J., Le Beau, M.M., Bloomfield, C.D., Cazzola, M., and Vardiman, J.W. The 2016 revision to the World Health Organization classification of myeloid neoplasms and acute leukemia. Blood. 2016;127(20):2391-2405. PubMed PMID: 27069254.
3. Rumi, E., and Cazzola, M. Diagnosis, risk stratification, and response evaluation in classical myeloproliferative neoplasms. Blood. 2017;129(6):680-692. PubMed PMID: 28028026; PMCID: PMC5335805.
4. Vainchenker, W., and Kralovics, R. Genetic basis and molecular pathophysiology of classical myeloproliferative neoplasms. Blood. 2017;129(6):667-679. PubMed PMID: 28028029.
5. Zoi, K., and Cross, N.C. Genomics of Myeloproliferative Neoplasms. J Clin Oncol. 2017;35(9):947-954. PubMed PMID: 28297629.
6. Bao, E.L., Nandakumar, S.K., Liao, X., Bick, A.G., Karjalainen, J., Tabaka, M., Gan, O.I., Havulinna, A.S., Kiiskinen, T.T.J., Lareau, C.A., de Lapuente Portilla, A.L., Li, B., Emdin, C., Codd, V., Nelson, C.P., Walker, C.J., Churchhouse, C., de la Chapelle, A., Klein, D.E., Nilsson, B., et al. Inherited myeloproliferative neoplasm risk affects haematopoietic stem cells. Nature. 2020;586(7831):769-775. Epub 2020/10/16. PubMed PMID: 33057200; PMCID: PMC7606745.
7. Marneth, A.E., and Mullally, A. The Molecular Genetics of Myeloproliferative Neoplasms. Cold Spring Harb Perspect Med. 2020;10(2). Epub 2019/09/25. PubMed PMID: 31548225; PMCID: PMC6996444.
8. Elf, S., Abdelfattah, N.S., Chen, E., Perales-Patón, J., Rosen, E.A., Ko, A., Peisker, F., Florescu, N., Giannini, S., Wolach, O., Morgan, E.A., Tothova, Z., Losman, J.-A., Schneider, R.K., Al-Shahrour, F., and Mullally, A. Mutant Calreticulin Requires Both Its Mutant C-terminus and the Thrombopoietin Receptor for Oncogenic Transformation. Cancer Discovery. 2016;6(4):368-381.
9. Vannucchi, A.M. Ruxolitinib versus standard therapy for the treatment of polycythemia vera. N Engl J Med. 2015;372(17):1670-1671. Epub 2015/04/23. PubMed PMID: 25901432.
10. Kleppe, M., Kwak, M., Koppikar, P., Riester, M., Keller, M., Bastian, L., Hricik, T., Bhagwat, N., McKenney, A.S., Papalexi, E., Abdel-Wahab, O., Rampal, R., Marubayashi, S., Chen, J.J., Romanet, V., Fridman, J.S., Bromberg, J., Teruya-Feldstein, J., Murakami, M., Radimerski, T., et al. JAK-STAT pathway activation in malignant and nonmalignant cells contributes to MPN pathogenesis and therapeutic response. Cancer Discov. 2015;5(3):316-331. Epub 2015/01/13. PubMed PMID: 25572172; PMCID: PMC4355105.
11. Deininger, M., Radich, J., Burn, T.C., Huber, R., Paranagama, D., and Verstovsek, S. The effect of long-term ruxolitinib treatment on JAK2p.V617F allele burden in patients with myelofibrosis. Blood. 2015;126(13):1551-1554. Epub 2015/08/01. PubMed PMID: 26228487; PMCID: PMC4582331.
12. Jutzi, J.S., Marneth, A.E., Ciboddo, M., Guerra-Moreno, A., Jimenez-Santos, M.J., Kosmidou, A., Dressman, J.W., Liang, H., Hamel, R., Lozano, P., Rumi, E., Doench, J.G., Gotlib, J., **Krishnan, A.**, Elf, S., Al-Shahrour, F., and Mullally, A. Whole-genome CRISPR screening identifies N-glycosylation as a genetic and therapeutic vulnerability in CALR-mutant MPNs. Blood. 2022;140(11):1291-1304. Epub 2022/06/29. PubMed PMID: 35763665.
13. Maxson, J.E. A new role for hematoxylin: targeting CALR. Blood. 2021;137(14):1848-1849. Epub 2021/04/09. PubMed PMID: 33830192.
14. Gerds, A.T. Beyond JAK-STAT: novel therapeutic targets in Ph-negative MPN. Hematology Am Soc Hematol Educ Program. 2019;2019(1):407-414. Epub 2019/12/07. PubMed PMID: 31808852; PMCID: PMC6913459 Celgene, Apexx Oncology, CTI Biopharma, and Inctye and research funding from Roche, Genentech, Incyte, Celgene, Imago Biosciences, Samus Therapeutics, and Gilead.

15. Jayavelu, A.K., Schnoder, T.M., Perner, F., Herzog, C., Meiler, A., Krishnamoorthy, G., Huber, N., Mohr, J., Edelmann-Stephan, B., Austin, R., Brandt, S., Palandri, F., Schroder, N., Isermann, B., Edlich, F., Sinha, A.U., Ungelenk, M., Hubner, C.A., Zeiser, R., Rahmig, S., et al. Splicing factor YBX1 mediates persistence of JAK2-mutated neoplasms. Nature. 2020;588(7836):157-163. Epub 2020/11/27. PubMed PMID: 33239784.
16. Lee, S.S., Verstovsek, S., and Pemmaraju, N. Novel Therapies in Myeloproliferative Neoplasms: Beyond JAK Inhibitor Monotherapy. J Immunother Precis Oncol. 2021;4(3):117-128. Epub 2022/06/07. PubMed PMID: 35663101; PMCID: PMC9138435.
17. How, J., Garcia, J.S., and Mullally, A. Biology and therapeutic targeting of molecular mechanisms in MPN. Blood. 2022. Epub 2022/12/20. PubMed PMID: 36534936.
18. Osorio, F.G., Soria-Valles, C., Santiago-Fernandez, O., Bernal, T., Mittelbrunn, M., Colado, E., Rodriguez, F., Bonzon-Kulichenko, E., Vazquez, J., Porta-de-la-Riva, M., Ceron, J., Fueyo, A., Li, J., Green, A.R., Freije, J.M., and Lopez-Otin, C. Loss of the proteostasis factor AIRAPL causes myeloid transformation by deregulating IGF-1 signaling. Nat Med. 2016;22(1):91-96. Epub 2015/12/23. PubMed PMID: 26692333.
19. LaFave, L.M., and Levine, R.L. Targeting a regulator of protein homeostasis in myeloproliferative neoplasms. Nat Med. 2016;22(1):20-21. Epub 2016/01/07. PubMed PMID: 26735404.
20. Shen, Z., Du, W., Perkins, C., Fechter, L., Natu, V., Maecker, H., Rowley, J., Gotlib, J., Zehnder, J., and Krishnan, A. Platelet transcriptome identifies progressive markers and potential therapeutic targets in chronic myeloproliferative neoplasms. Cell Reports Medicine. 2021;2(10):100425; PMCID: PMC8561315.
21. Jain, K., Tyagi, T., Du, J., Hu, X., Patell, K., Martin, K.A., and Hwa, J. Unfolded Protein Response Differentially Modulates the Platelet Phenotype. Circulation research. 2022;131(4):290-307. Epub 2022/07/22. PubMed PMID: 35862006; PMCID: PMC9357223.
22. Kaushik, S., and Cuervo, A.M. Proteostasis and aging. Nature Medicine. 2015;21(12):1406-1415.
23. Costa-Mattioli, M., and Walter, P. The integrated stress response: From mechanism to disease. Science. 2020;368(6489).
24. Walter, P., and Ron, D. The unfolded protein response: from stress pathway to homeostatic regulation. Science. 2011;334(6059):1081-1086.
25. Lebeaupin, C., Yong, J., and Kaufman, R.J. The impact of the ER unfolded protein response on cancer initiation and progression: therapeutic implications. Adv Exp Med Biol. 2020;1243:113-131; PMCID: PMC7243802.
26. Sutton, K.A., Jungnickel, M.K., Wang, Y., Cullen, K., Lambert, S., and Florman, H.M. Enkurin is a novel calmodulin and TRPC channel binding protein in sperm. Dev Biol. 2004;274(2):426-435. Epub 2004/09/24. PubMed PMID: 15385169.
27. Wright, J.R., Amisten, S., Goodall, A.H., and Mahaut-Smith, M.P. Transcriptomic analysis of the ion channelome of human platelets and megakaryocytic cell lines. Thromb Haemost. 2016;116(2):272-284. Epub 2016/06/10. PubMed PMID: 27277069; PMCID: PMC5080539.
28. Authi, K.S. TRP channels in platelet function. Handb Exp Pharmacol. 2007(179):425-443. Epub 2007/01/16. PubMed PMID: 17217071.
29. Jungnickel, M.K., Sutton, K.A., Baker, M.A., Cohen, M.G., Sanderson, M.J., and Florman, H.M. The flagellar protein Enkurin is required for mouse sperm motility and for transport through the female reproductive tract. Biol Reprod. 2018;99(4):789-797. Epub 2018/05/08. PubMed PMID: 29733335; PMCID: PMC6203878.
30. Fucikova, J., Spisek, R., Kroemer, G., and Galluzzi, L. Calreticulin and cancer. Cell Res. 2021;31(1):5-16. Epub 2020/08/01. PubMed PMID: 32733014; PMCID: PMC7853084.
31. Klampfl, T., Gisslinger, H., Harutyunyan, A.S., Nivarthi, H., Rumi, E., Milosevic, J.D., Them, N.C., Berg, T., Gisslinger, B., Pietra, D., Chen, D., Vladimer, G.I., Bagienski, K., Milanesi, C., Casetti, I.C.,

Sant'Antonio, E., Ferretti, V., Elena, C., Schischlik, F., Cleary, C., et al. Somatic mutations of calreticulin in myeloproliferative neoplasms. N Engl J Med. 2013;369(25):2379-2390. Epub 2013/12/12. PubMed PMID: 24325356.

32. Merlinsky, T.R., Levine, R.L., and Pronier, E. Unfolding the Role of Calreticulin in Myeloproliferative Neoplasm Pathogenesis. Clin Cancer Res. 2019;25(10):2956-2962. Epub 2019/01/19. PubMed PMID: 30655313; PMCID: PMC6522317.

33. Prins, D., González Arias, C., Klampfl, T., Grinfeld, J., and Green, A.R. Mutant Calreticulin in the Myeloproliferative Neoplasms. HemaSphere. 2020;4(1):e333.

34. Michalak, M., Groenendyk, J., Szabo, E., Gold, L.I., and Opas, M. Calreticulin, a multi-process calcium-buffering chaperone of the endoplasmic reticulum. Biochem J. 2009;417(3):651-666. Epub 2009/01/13. PubMed PMID: 19133842.

35. Clapham, D.E. Calcium Signaling. Cell. 2007;131(6):1047-1058.

36. Tonelli, F.M.P., Santos, A.K., Gomes, D.A., da Silva, S.L., Gomes, K.N., Ladeira, L.O., and Resende, R.R. (2012). Stem Cells and Calcium Signaling. In Calcium Signaling, M.S. Islam, ed. (Springer Netherlands), pp. 891-916.

37. Andrea Di Buduo, C., Moccia, F., Battiston, M., De Marco, L., Mazzucato, M., Moratti, R., Tanzi, F., and Balduini, A. The importance of calcium in the regulation of megakaryocyte function. Haematologica. 2014;99(4):769-778.

38. Salati, S., Prudente, Z., Genovese, E., Pennucci, V., Rontauroli, S., Bartalucci, N., Mannarelli, C., Ruberti, S., Zini, R., Rossi, C., Bianchi, E., Guglielmelli, P., Tagliafico, E., Vannucchi, A.M., and Manfredini, R. Calreticulin Affects Hematopoietic Stem/Progenitor Cell Fate by Impacting Erythroid and Megakaryocytic Differentiation. Stem Cells Dev. 2018;27(4):225-236. Epub 2017/12/21. PubMed PMID: 29258411.

39. Chan, C.-P., Kok, K.-H., and Jin, D.-Y. CREB3 subfamily transcription factors are not created equal: Recent insights from global analyses and animal models. Cell Biosci. 2011;1(1):6; PMCID: PMC3116243.

40. Cui, M., Kanemoto, S., Cui, X., Kaneko, M., Asada, R., Matsuhisa, K., Tanimoto, K., Yoshimoto, Y., Shukunami, C., and Imaizumi, K. OASIS modulates hypoxia pathway activity to regulate bone angiogenesis. Sci Rep. 2015;5:16455; PMCID: PMC4642342.

41. García, I.A., Torres Demichelis, V., Viale, D.L., Di Giusto, P., Ezhova, Y., Polishchuk, R.S., Sampieri, L., Martinez, H., Sztul, E., and Alvarez, C. CREB3L1-mediated functional and structural adaptation of the secretory pathway in hormone-stimulated thyroid cells. J Cell Sci. 2017;130(24):4155-4167; PMCID: PMC6518157.

42. Sampieri, L., Di Giusto, P., and Alvarez, C. CREB3 Transcription Factors: ER-Golgi Stress Transducers as Hubs for Cellular Homeostasis. Front Cell Dev Biol. 2019;7:123; PMCID: PMC6616197.

43. Schrock, M.S., Stromberg, B.R., Scarberry, L., and Summers, M.K. APC/C ubiquitin ligase: Functions and mechanisms in tumorigenesis. Semin Cancer Biol. 2020;67(Pt 2):80-91. Epub 2020/03/14. PubMed PMID: 32165320; PMCID: PMC7483777.

44. Visintin, R., Prinz, S., and Amon, A. CDC20 and CDH1: a family of substrate-specific activators of APC-dependent proteolysis. Science. 1997;278(5337):460-463. Epub 1997/10/23. PubMed PMID: 9334304.

45. Yu, H. Cdc20: A WD40 Activator for a Cell Cycle Degradation Machine. Molecular Cell. 2007;27(1):3-16.

46. Campbell, R.A., Franks, Z., Bhatnagar, A., Rowley, J.W., Manne, B.K., Supiano, M.A., Schwertz, H., Weyrich, A.S., and Rondina, M.T. Granzyme A in human platelets regulates the synthesis of proinflammatory cytokines by monocytes in aging. J Immunol. 2018;200(1):295-304; PMCID: PMC5736423.

47. Rowley, J.W., Oler, A.J., Tolley, N.D., Hunter, B.N., Low, E.N., Nix, D.A., Yost, C.C., Zimmerman, G.A., and Weyrich, A.S. Genome-wide RNA-seq analysis of human and mouse platelet transcriptomes. Blood. 2011;118(14):e101-111. Epub 2011/05/21. PubMed PMID: 21596849; PMCID: PMC3193274.
48. Middleton, E.A., Rowley, J.W., Campbell, R.A., Grissom, C.K., Brown, S.M., Beesley, S.J., Schwertz, H., Kosaka, Y., Manne, B.K., Krauel, K., Tolley, N.D., Eustes, A.S., Guo, L., Paine, R., 3rd, Harris, E.S., Zimmerman, G.A., Weyrich, A.S., and Rondina, M.T. Sepsis alters the transcriptional and translational landscape of human and murine platelets. Blood. 2019;134(12):911-923. Epub 2019/08/02. PubMed PMID: 31366617; PMCID: PMC6753624.
49. Amisten, S. A rapid and efficient platelet purification protocol for platelet gene expression studies. Methods in molecular biology (Clifton, N.J.). 2012;788:155-172. Epub 2011/12/02. PubMed PMID: 22130707.
50. Edelstein, L.C., Simon, L.M., Montoya, R.T., Holinstat, M., Chen, E.S., Bergeron, A., Kong, X., Nagalla, S., Mohandas, N., Cohen, D.E., Dong, J.-f., Shaw, C., and Bray, P.F. Racial differences in human platelet PAR4 reactivity reflect expression of PCTP and miR-376c. Nature Medicine. 2013;19(12):1609-1616.
51. Bhatlekar, S., Basak, I., Edelstein, L.C., Campbell, R.A., Lindsey, C.R., Italiano, J.E., Weyrich, A.S., Rowley, J.W., Rondina, M.T., Sola-Visner, M., and Bray, P.F. Anti-apoptotic BCL2L2 increases megakaryocyte proplatelet formation in cultures of human cord blood. Haematologica. 2019;104(10):2075-2083.
52. Khan, I., Huang, Z., Wen, Q., Stankiewicz, M.J., Gilles, L., Goldenson, B., Schultz, R., Diebold, L., Gurbuxani, S., Finke, C.M., Lasho, T.L., Koppikar, P., Pardanani, A., Stein, B., Altman, J.K., Levine, R.L., Tefferi, A., and Crispino, J.D. AKT is a therapeutic target in myeloproliferative neoplasms. Leukemia. 2013;27(9):1882-1890. Epub 2013/06/12. PubMed PMID: 23748344; PMCID: PMC4023863.
53. Fruman, D.A., Chiu, H., Hopkins, B.D., Bagrodia, S., Cantley, L.C., and Abraham, R.T. The PI3K Pathway in Human Disease. Cell. 2017;170(4):605-635.
54. Song, M., Bode, A.M., Dong, Z., and Lee, M.-H. AKT as a Therapeutic Target for Cancer. Cancer Research. 2019;79(6):1019-1031.
55. Yang, J., Nie, J., Ma, X., Wei, Y., Peng, Y., and Wei, X. Targeting PI3K in cancer: mechanisms and advances in clinical trials. Mol Cancer. 2019;18(1):26.
56. Liu, L., Inoki, A., Fan, K., Mao, F., Shi, G., Jin, X., Zhao, M., Ney, G., Jones, M.A., Sun, S., Dou, Y., Inoki, K., Qi, L., and Li, Q. ER associated degradation preserves hematopoietic stem cell quiescence and self-renewal by restricting mTOR activity. Blood. 2020. Epub 2020/11/06. PubMed PMID: 33150381.
57. Skov, V., Larsen, T.S., Thomassen, M., Riley, C., Jensen, M.K., Bjerrum, O.W., Kruse, T.A., and Hasselbalch, H.C. Increased Expression of Proteasome-Related Genes In Patients with Primary Myelofibrosis. Blood. 2010;116(21):4117-4117.
58. Deininger, M., Radich, J., Burn, T.C., Huber, R., Paranagama, D., and Verstovsek, S. The effect of long-term ruxolitinib treatment on JAK2p.V617F allele burden in patients with myelofibrosis. Blood. 2015;126(13):1551-1554.
59. VanGenderen, C., Harkness, T.A.A., and Arnason, T.G. The role of Anaphase Promoting Complex activation, inhibition and substrates in cancer development and progression. Aging (Albany NY). 2020;12(15):15818-15855. Epub 2020/08/18. PubMed PMID: 32805721; PMCID: PMC7467358.
60. Spivak, J.L., Jie, C., Williams, D., and Moliterno, A.R. JAK2V671F, Gender and the Gene Expression Profile of Polycythemia Vera. Blood. 2008;112(11):2805-2805.
61. Nangalia, J., Massie, C.E., Baxter, E.J., Nice, F.L., Gundem, G., Wedge, D.C., Avezov, E., Li, J., Kollmann, K., Kent, D.G., Aziz, A., Godfrey, A.L., Hinton, J., Martincorena, I., Van Loo, P., Jones, A.V., Guglielmelli, P., Tarpey, P., Harding, H.P., Fitzpatrick, J.D., et al. Somatic CALR mutations in myeloproliferative neoplasms with nonmutated JAK2. N Engl J Med. 2013;369(25):2391-2405. Epub 2013/12/12. PubMed PMID: 24325359; PMCID: PMC3966280.

62. Di Buduo, C.A., Abbonante, V., Marty, C., Moccia, F., Rumi, E., Pietra, D., Soprano, P.M., Lim, D., Cattaneo, D., Iurlo, A., Gianelli, U., Barosi, G., Rosti, V., Plo, I., Cazzola, M., and Balduini, A. Defective interaction of mutant calreticulin and SOCE in megakaryocytes from patients with myeloproliferative neoplasms. Blood. 2020;135(2):133-144. Epub 2019/11/08. PubMed PMID: 31697806; PMCID: PMC6952826.
63. Mullally, A. Both sides now: losses and gains of mutant CALR. Blood. 2020;135(2):82-83. Epub 2020/01/10. PubMed PMID: 31917838; PMCID: PMC6952827.
64. Geyer, H.L., Dueck, A.C., Scherber, R.M., and Mesa, R.A. Impact of inflammation on myeloproliferative neoplasm symptom development. Mediators Inflamm. 2015;2015:284706; PMCID: PMC4619953.
65. Koschmieder, S., and Chatain, N. Role of inflammation in the biology of myeloproliferative neoplasms. Blood Rev. 2020;42:100711. Epub 2020/06/09. PubMed PMID: 32505517.
66. Vainchenker, W., Leroy, E., Gilles, L., Marty, C., Plo, I., and Constantinescu, S.N. JAK inhibitors for the treatment of myeloproliferative neoplasms and other disorders. F1000Res. 2018;7:82. Epub 2018/02/06. PubMed PMID: 29399328; PMCID: PMC5773931.
67. Woods, B., Chen, W., Chiu, S., Marinaccio, C., Fu, C., Gu, L., Bulic, M., Yang, Q., Zouak, A., Jia, S., Suraneni, P.K., Xu, K., Levine, R.L., Crispino, J.D., and Wen, Q.J. Activation of JAK/STAT Signaling in Megakaryocytes Sustains Myeloproliferation In Vivo. Clin Cancer Res. 2019;25(19):5901-5912. Epub 2019/06/21. PubMed PMID: 31217200; PMCID: PMC6774846.
68. Bruno, S., Ghelli Luserna di Rora, A., Napolitano, R., Soverini, S., Martinelli, G., and Simonetti, G. CDC20 in and out of mitosis: a prognostic factor and therapeutic target in hematological malignancies. J Exp Clin Cancer Res. 2022;41(1):159. Epub 2022/05/01. PubMed PMID: 35490245; PMCID: PMC9055704.

Tables

Table 1: Summary of all cell types used, their sources and the respective analyses performed.

Table 1: Experimental Framework and Components							
#	**Cell type**	**Source**	**Megakaryocyte (MK) culture**	**ENKUR silencing**	**ER stress induction**	**RNA expression (MK and/or Platelet)**	**Protein expression (MK and/or Platelet)**
1	Platelets	Peripheral blood (n = 49)				X *CALR, CREB3L1, CDC20, ENKUR*	X CALR, CREB3L1, CDC20, ENKUR
2	$CD34^+$	Bone marrow (n = 8)	X			X *CALR, CREB3L1, CDC20, ENKUR*	
3	$CD34^+$	Cord blood (n = 4)	X	X		X *CALR, CREB3L1, CDC20, ENKUR*	X CALR, CREB3L1, CDC20, ENKUR, PI3K and Akt
4	$CD34^+$	Peripheral blood (n = 7)	X	X	X	X *CALR, CREB3L1, CDC20, ENKUR*	X CALR, CREB3L1, CDC20, ENKUR, PI3K and Akt

Figure Legends

Figure 1: RNA expression in platelets and whole blood of MPN patients and protein expression in platelets

(A) MPN Platelet RNA-seq normalized expression data: MPN patients (total n=99: ET n=24; PV n=33; MF n=42) vs healthy donors (n=21) (B) whole blood RNA: MPN patients (total n=109: ET n=39; PV n=38; MF n=32) vs healthy donors (n=10) (C) platelet protein: peripheral blood platelets were isolated from MPN patients (total n=38: MF n=12; PV n=19; ET n=7) and healthy donors (n=11). Bonferroni multiple comparisons adjusted p values ****$p<0.0001$, ***$p<0.001$ and **$p<0.01$ when compared with controls (healthy donors). All RNA expression is normalized to GAPDH and expressed as log2 fold change.

Figure 2: Culturing of $CD34^+$ cells from the bone marrow of MPN patients and RNA expression

(A) Microscopic images of the $CD34^+$ cells isolated from the bone marrow of MPN patients over the 15-day culture period at 20X magnification. Notice the formation of megakaryocytes indicated by the red arrow. (B) Flow cytometric analysis of cell surface markers to confirm the production of megakaryocyte and platelet fractions after 15 days of culture. (C) megakaryocytic RNA: cell culture from fresh MPN patient bone marrow (n=8) derived $CD34^+$ cells then differentiated over 15 days into megakaryocytes. All RNA expression is normalized to GAPDH and expressed as log2 fold change. Bonferroni adjusted p values **$p<0.01$, *$p<0.05$.

Figure 3: Experimental design and workflow of Lentiviral transduction-induced silencing of ENKUR gene in $CD34^+$ stem cells

(A) Workflow of the shRNA construction and generation of the lentivirus (B) experimental plan for the silencing of the ENKUR gene in $CD34^+$ stem cells. The $CD34^+$ cells were isolated from both peripheral and cord blood.

Figure 4: Lentiviral transduction induced silencing of ENKUR gene in CD34$^+$ stem cells

(A) Flow cytometric analysis of cell surface markers to confirm the megakaryocytic and platelet fractions after 15 days of culture. (B) RNA expression levels in the CD34$^+$ cell-derived megakaryocytes and platelets. (C) (i) Western blot of the CD34$^+$ cells derived megakaryocytes (n=4 cord blood and n=4 peripheral blood) and (ii) densitometry for the blots. Densitometry was performed using the IVIS imaging software ($^{****}p<0.0001$, $^{***}p<0.001$, $^{**}p<0.01$ and $^{*}p<0.05$ when compared with non-silenced controls).

Figure 5: Effect of ER stress on Megs derived from CD34$^+$ cells from healthy donors

(A) Representative microscopic images of the CD34$^+$ cells isolated from the peripheral blood of healthy donors over the 15-day culture period at 20X magnification. The ER stressor, thapsigargin (125nM) was added to the culture at day 7 and cultured for another 7 days. (B) RNA expression: cell culture from thapsigargin-treated CD34$^+$ derived megakaryocytes (n=7). (C) (i) Western blot of the thapsigargin-treated CD34$^+$ cells derived megakaryocytes (n=3 in triplicate) and (ii) densitometry for the blots. Densitometry was performed using the ImageJ software ($^{****}p<0.0001$,$^{**}p<0.01$ when compared with untreated controls).

Figure 6: Probable mechanism for the role of *ENKUR* downregulation in cell proliferation

We hypothesize that, under normal conditions, enkurin at sufficient physiological levels is bound to PI3K via the SH3 binding domain, thus regulating its activation[26]. However, in the setting of MPNs, downregulation of enkurin likely contributes to free PI3K and its prolonged activation, further activating Akt and potentially other signaling mechanisms prompting overexpression of cell differentiation cycle genes including CDC20[68] and cell proliferation.

Supplementary Figure legends

Figure S1: RNA expression in platelets and whole blood of MPN patients and protein expression in platelets

(A) MPN Platelet RNA-seq Normalized Expression Data: MPN patients (n=99: ET n=24; PV n=33; MF n=42) vs healthy donors (n=21) (B) whole blood RNA: MPN patients (n=109: ET n=39; PV n=38; MF n=32) vs healthy donors (n=10) (C) platelet protein: peripheral blood platelets were isolated from MPN patients (n=38: MF n=12; PV n=19; ET n=7) and healthy donors (n=11).

Figure S2: Culturing of $CD34^+$ cells from the bone marrow of MPN patients and RNA expression

(A) Confocal microscopy: Microscopic images of the $CD34^+$ cells isolated from the bone marrow of MPN patients over the 15-day culture period at 20X magnification. The cells were treated with cell surface markers for $CD34^+$ cells (CD34), Megakaryocytes (CD41, CD42b, and CD61) (B) Quantification of $CD41^+$ megakaryocytes from $CD34^+$ cells isolated from the bone marrow of MPN patients over the 15-day culture period (C) Megakaryocytic RNA: cell culture from fresh MPN patient bone marrow (n=8) derived $CD34^+$ cells then differentiated over 15 days into megakaryocytes. All RNA expression is normalized to GAPDH and expressed as log2 fold change.

Figure S3: Effect of Lentiviral transduction induced silencing of ENKUR gene on CALR and CREB3L1 gene expression in $CD34^+$ stem cells

(A) RNA expression levels in the $CD34^+$ cell-derived megakaryocytes and platelets. Log2 fold change was plotted by normalizing with the control (B) (i) Western blot of the $CD34^+$ cell-derived megakaryocytes (n=4 cord blood and n=4 peripheral blood) and (ii) densitometry for the blots. Densitometry was performed using IVIS imaging software.

FIGURE 1

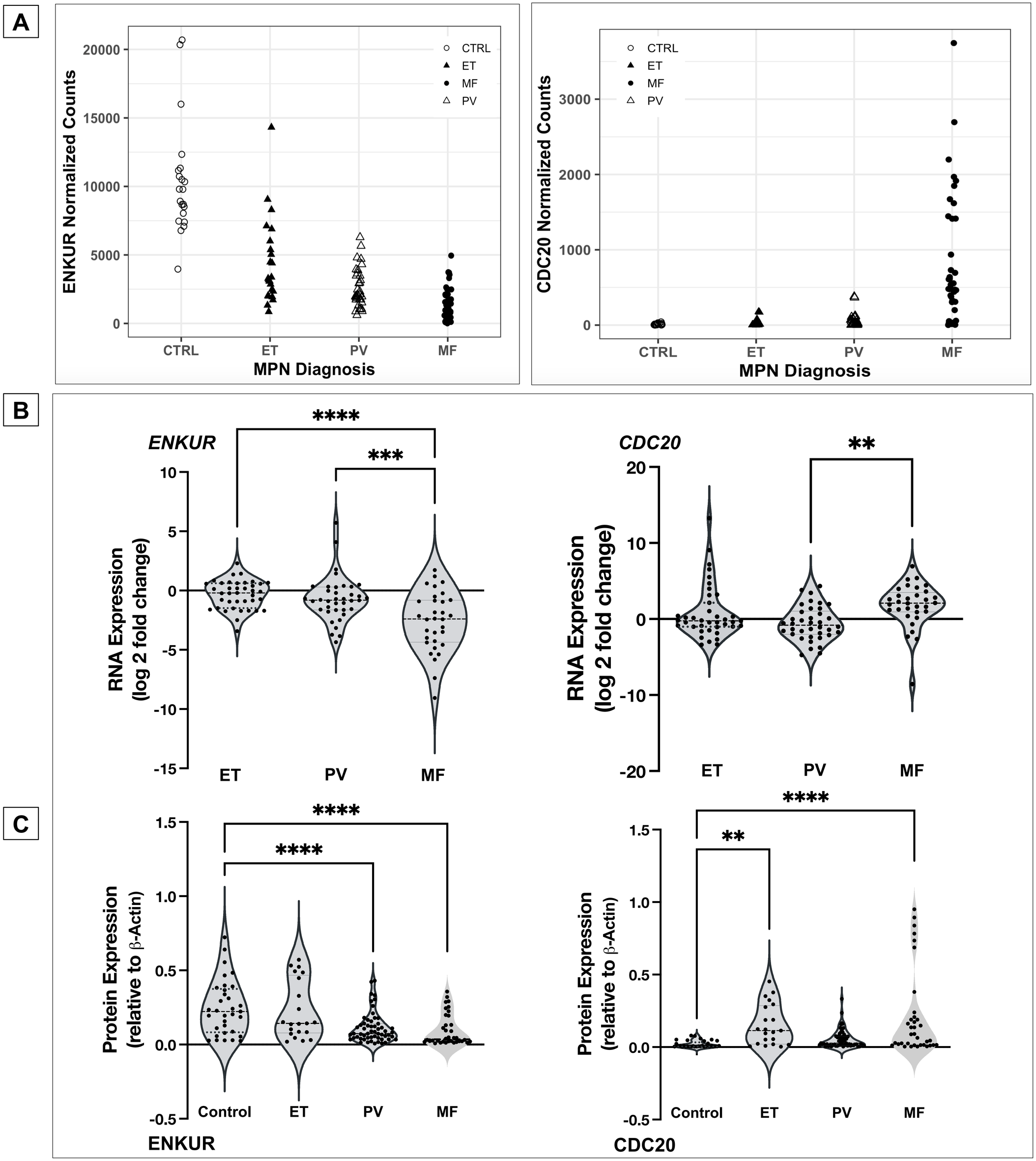
A
ENKUR Normalized Counts
20000
15000
10000
5000
0
CTRL
ET
MF
PV
MPN Diagnosis
CDC20 Normalized Counts
3000
2000
1000
B
ENKUR
****
***
RNA Expression
(log 2 fold change)
10
5
-5
-10
-15
CDC20
**
20
-20
C
Protein Expression
(relative to β-Actin)
1.5
1.0
0.5
0.0
-0.5
Control
ENKUR
CDC20

FIGURE 2

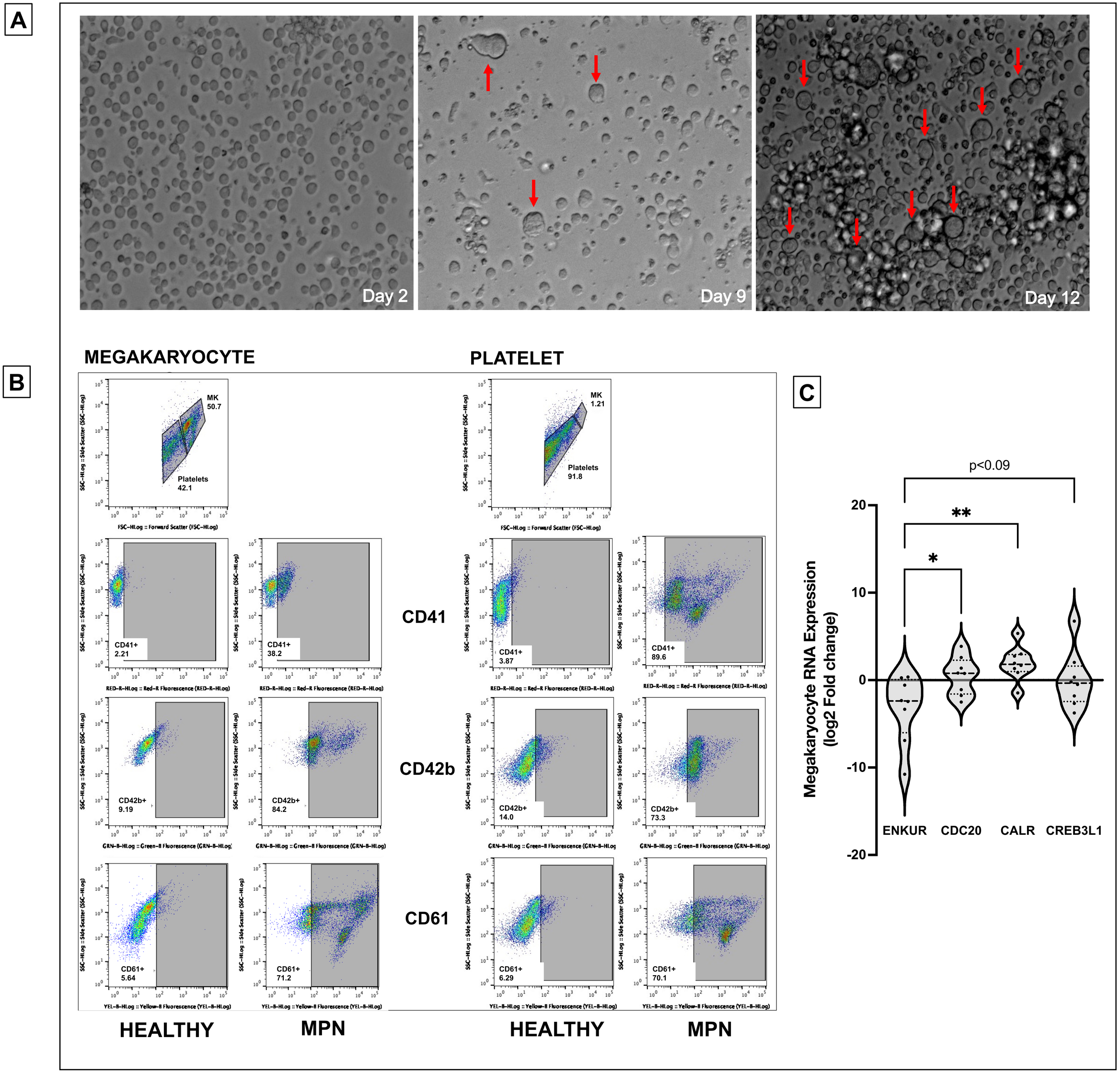
A
Day 2
Day 9
Day 12
B
MEGAKARYOCYTE
PLATELET
MK 50.7
Platelets 42.1
MK 1.21
Platelets 91.8
CD41
CD41+ 2.21
CD41+ 38.2
CD41+ 3.87
CD41+ 89.6
CD42b
CD42b+ 9.19
CD42b+ 84.2
CD42b+ 14.0
CD42b+ 73.3
CD61
CD61+ 5.64
CD61+ 71.2
CD61+ 6.29
CD61+ 70.1
HEALTHY
MPN
HEALTHY
MPN
C
p<0.09
**
*
Megakaryocyte RNA Expression (log2 Fold change)
20
10
0
-10
-20
ENKUR
CDC20
CALR
CREB3L1

FIGURE 3

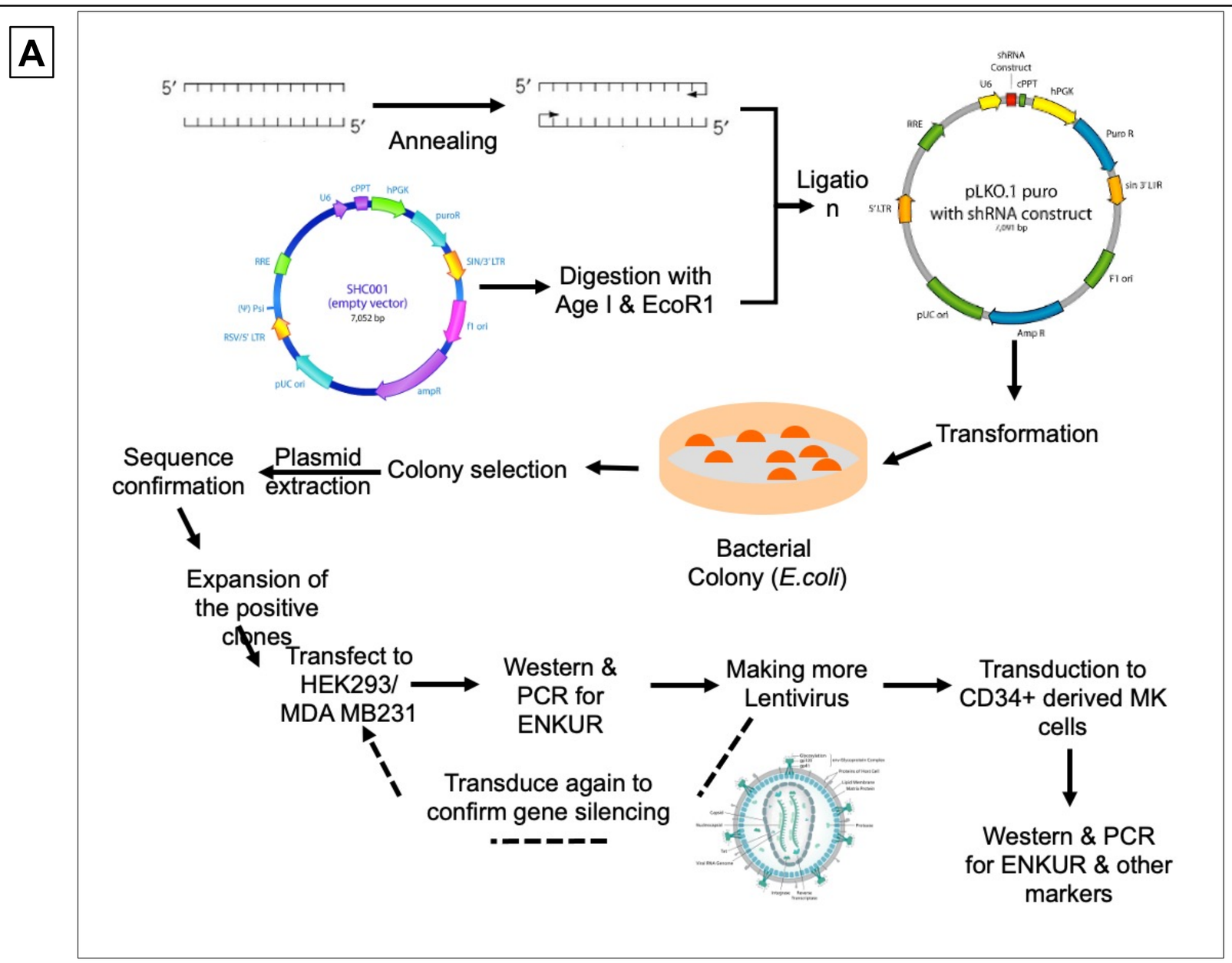
A
5′
5′
Annealing
5′
5′
Ligation
shRNA Construct
U6
cPPT
hPGK
Puro R
sin 3′ LTR
F1 ori
Amp R
pUC ori
5′ LTR
RRE
pLKO.1 puro
with shRNA construct
U6
cPPT
hPGK
puroR
SIN/3′ LTR
f1 ori
ampR
pUC ori
RSV/5′ LTR
(Ψ) Psi
RRE
SHC001
(empty vector)
7,052 bp
Digestion with
Age I & EcoR1
Transformation
Bacterial
Colony (E.coli)
Colony selection
Plasmid
extraction
Sequence
confirmation
Expansion of
the positive
clones
Transfect to
HEK293/
MDA MB231
Western &
PCR for
ENKUR
Making more
Lentivirus
Transduction to
CD34+ derived MK
cells
Transduce again to
confirm gene silencing
Western & PCR
for ENKUR & other
markers

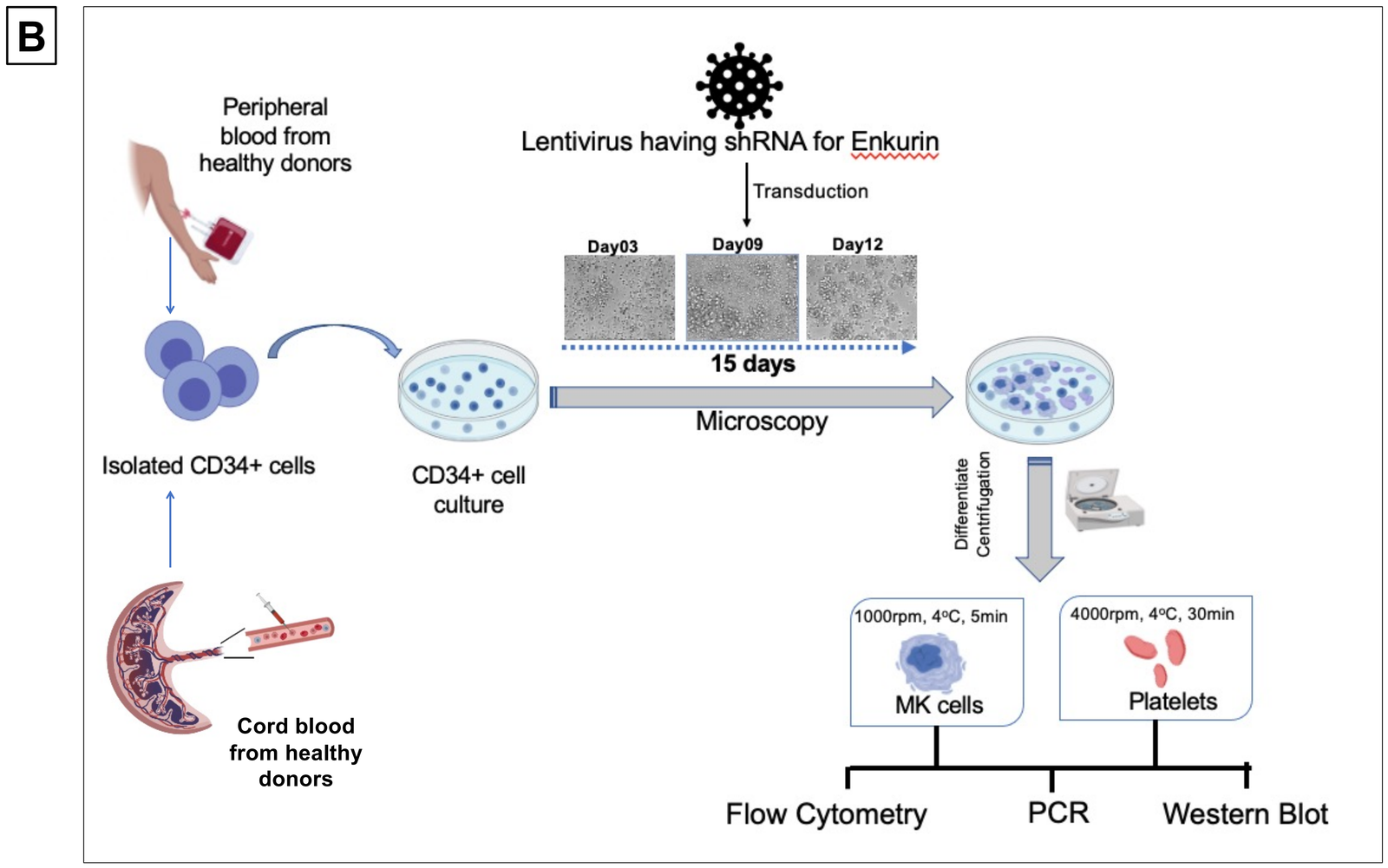
B
Peripheral
blood from
healthy donors
Lentivirus having shRNA for Enkurin
Transduction
Day03
Day09
Day12
15 days
Microscopy
Isolated CD34+ cells
CD34+ cell
culture
Differentiate
Centrifugation
1000rpm, 4ºC, 5min
MK cells
4000rpm, 4ºC, 30min
Platelets
Cord blood
from healthy
donors
Flow Cytometry
PCR
Western Blot

FIGURE 4

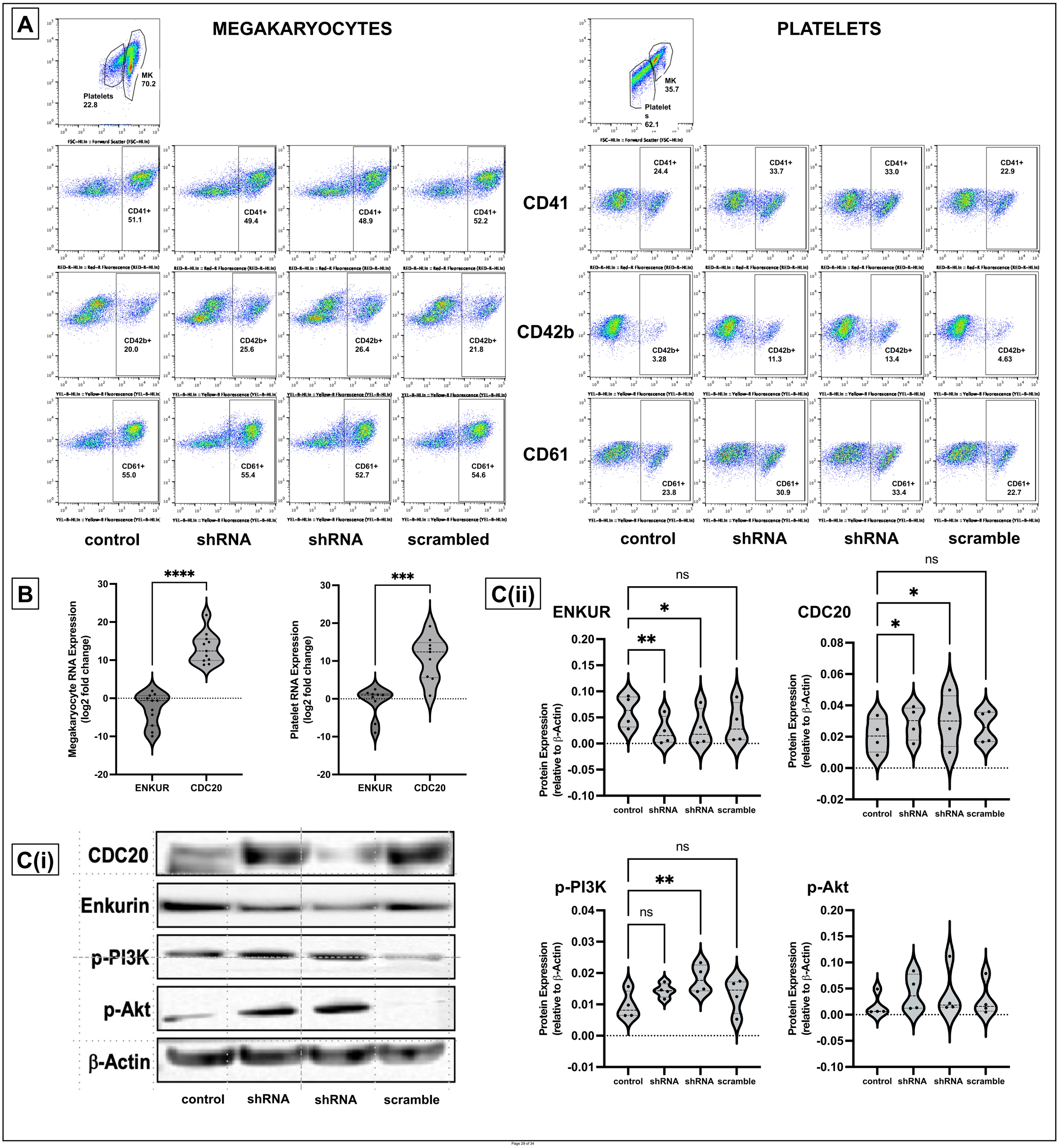
A
MEGAKARYOCYTES
PLATELETS
MK 70.2
Platelets 22.8
MK 35.7
Platelets 62.1
CD41
CD42b
CD61
CD41+ 51.1
CD41+ 49.4
CD41+ 48.9
CD41+ 52.2
CD41+ 24.4
CD41+ 33.7
CD41+ 33.0
CD41+ 22.9
CD42b+ 20.0
CD42b+ 25.6
CD42b+ 26.4
CD42b+ 21.8
CD42b+ 3.28
CD42b+ 11.3
CD42b+ 13.4
CD42b+ 4.63
CD61+ 55.0
CD61+ 55.4
CD61+ 52.7
CD61+ 54.6
CD61+ 23.8
CD61+ 30.9
CD61+ 33.4
CD61+ 22.7
control
shRNA
shRNA
scrambled
control
shRNA
shRNA
scramble
B
Megakaryocyte RNA Expression (log2 fold change)
Platelet RNA Expression (log2 fold change)
****
***
ENKUR
CDC20
C(ii)
ENKUR
CDC20
p-PI3K
p-Akt
Protein Expression (relative to β-Actin)
ns
*
**
control
shRNA
shRNA
scramble
C(i)
CDC20
Enkurin
p-PI3K
p-Akt
β-Actin
control
shRNA
shRNA
scramble

FIGURE 5

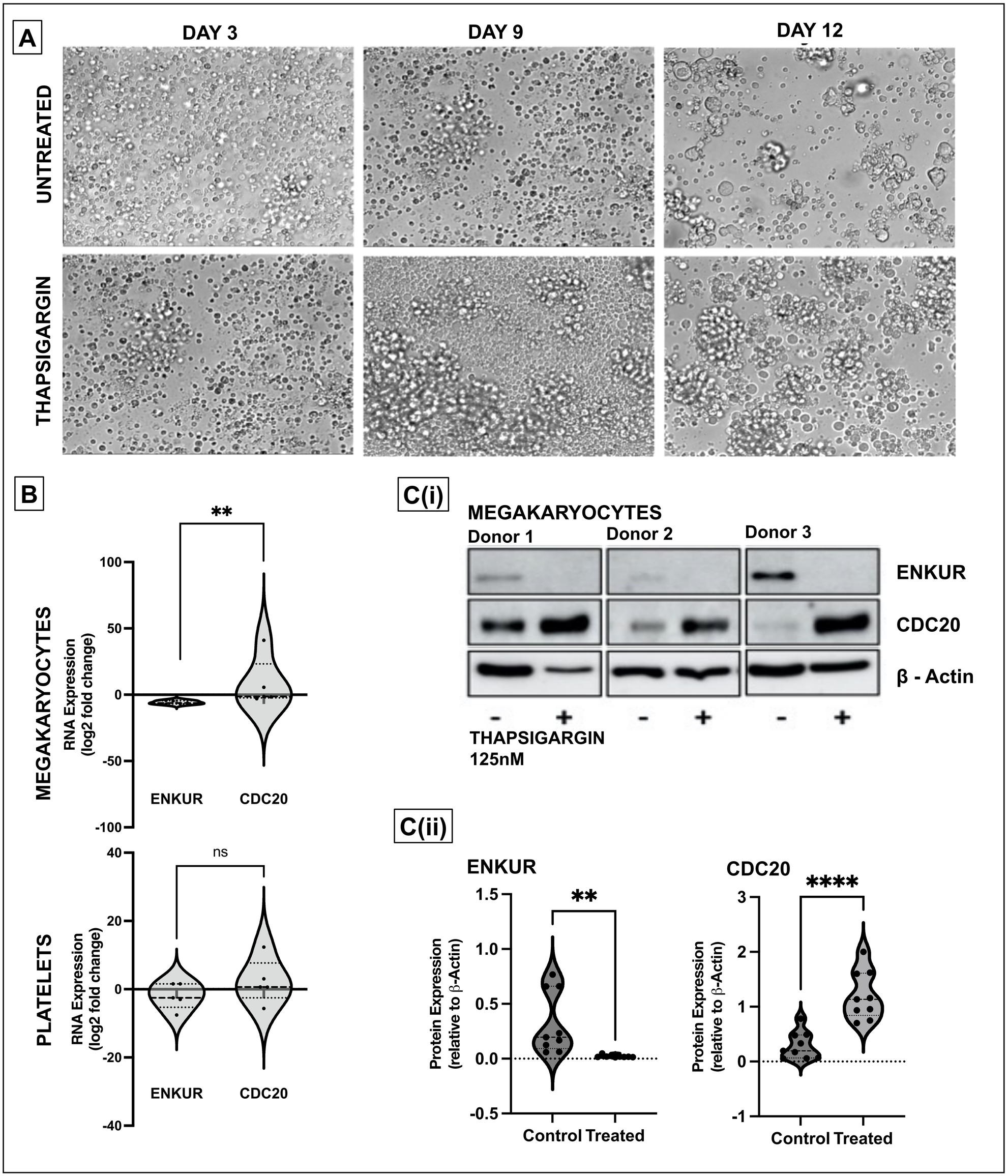
A
DAY 3
DAY 9
DAY 12
UNTREATED
THAPSIGARGIN
B
MEGAKARYOCYTES
RNA Expression (log2 fold change)
**
100
50
0
-50
-100
ENKUR
CDC20
PLATELETS
RNA Expression (log2 fold change)
ns
40
20
0
-20
-40
ENKUR
CDC20
C(i)
MEGAKARYOCYTES
Donor 1
Donor 2
Donor 3
ENKUR
CDC20
β - Actin
- + - + - +
THAPSIGARGIN 125nM
C(ii)
ENKUR
**
Protein Expression (relative to β-Actin)
1.5
1.0
0.5
0.0
-0.5
Control Treated
CDC20
****
Protein Expression (relative to β-Actin)
3
2
1
0
-1
Control Treated

FIGURE 6

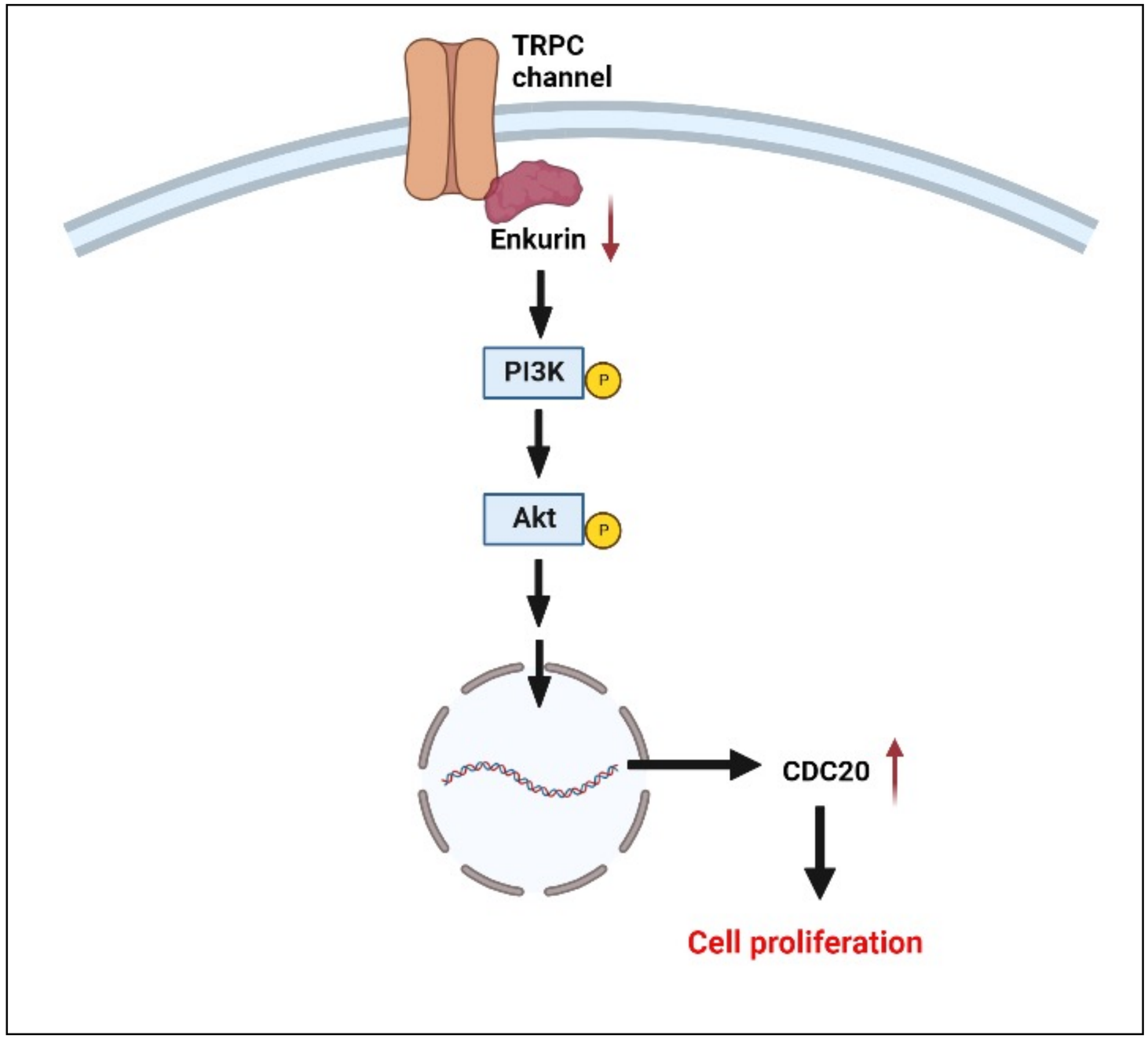

SUPPLEMENTARY FIGURE 1

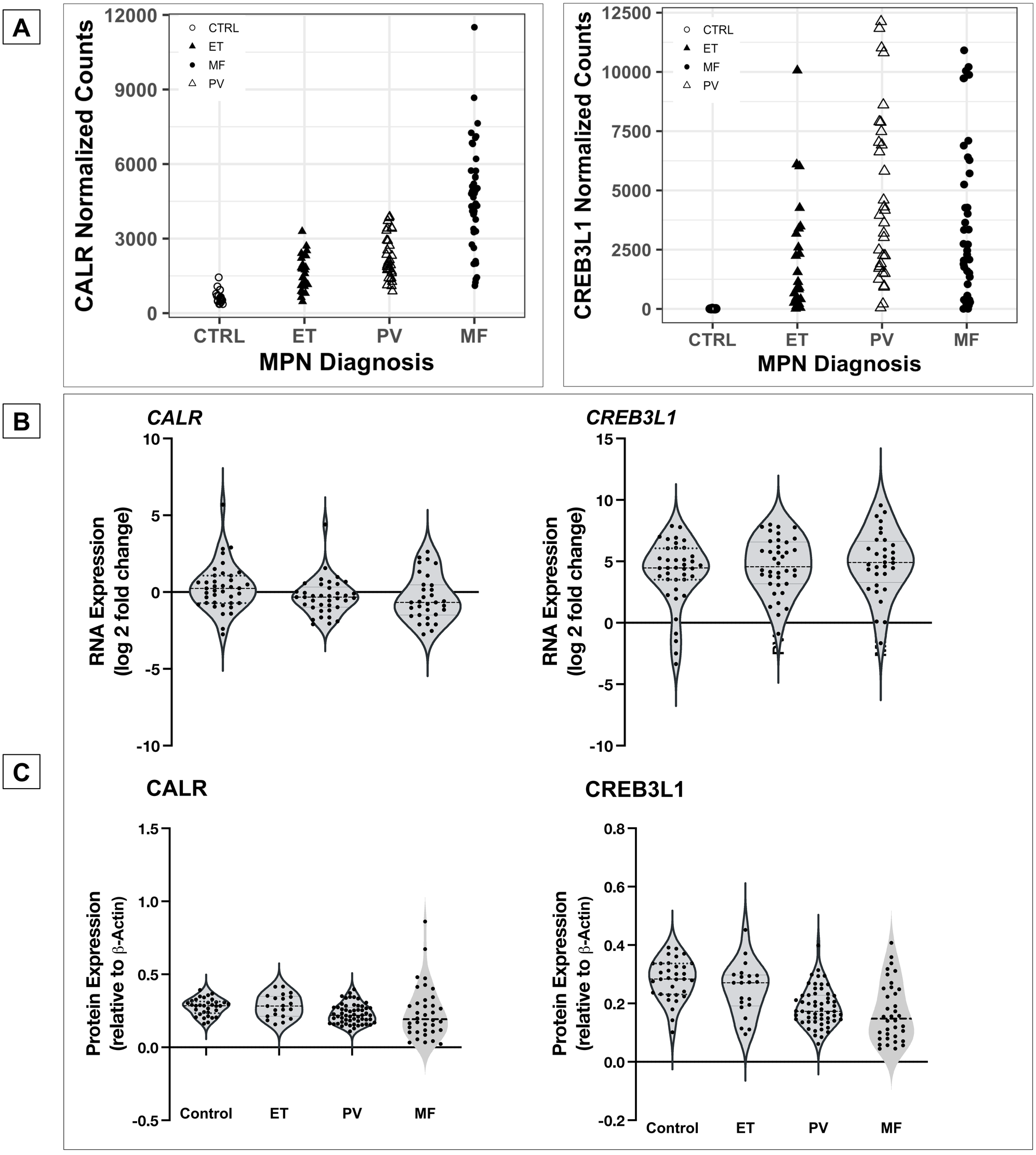

SUPPLEMENTARY FIGURE 2

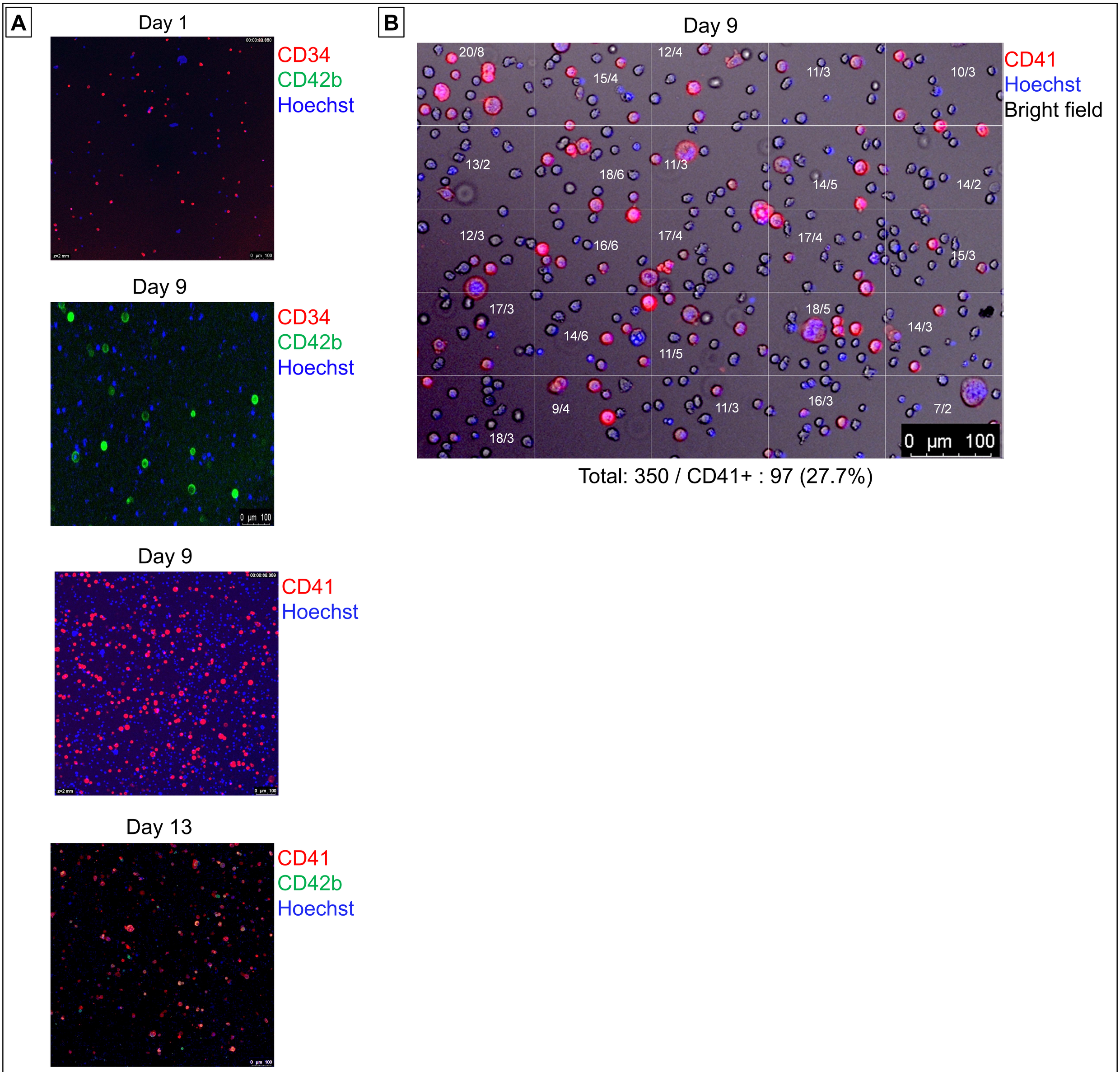
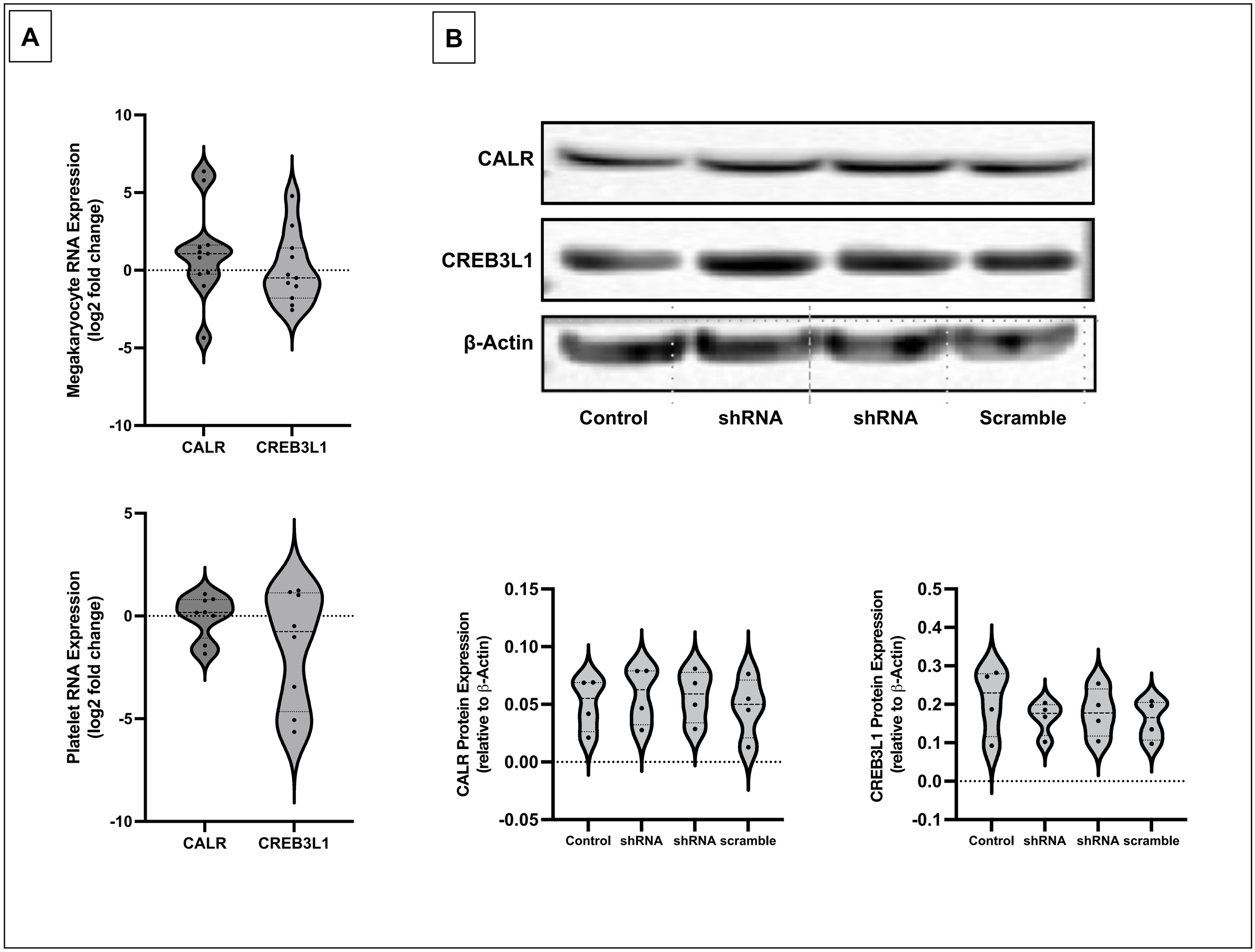
SUPPLEMENTARY FIGURE 3